Oussama Khatib
Robotics Laboratory
Department of Computer Science
Stanford University
Stanford, CA 94305
E-mail: khatib@cs.stanford.edu

Inertial Properties in Robotic Manipulation: An Object-Level Framework

Abstract

Consideration of dynamics is critical in the analysis, design, and control of robot systems. This article presents an extensive study of the dynamic properties of several important classes of robotic structures and proposes a number of general dynamic strategies for their coordination and control. This work is a synthesis of both previous and new results developed within the task-oriented operational space formulation. Here we introduce a unifying framework for the analysis and control of robotic systems, beginning with an analysis of inertial properties based on two models that independently describe the mass and inertial characteristics associated with linear and angular motions. To visualize these properties, we propose a new geometric representation, termed the belted ellipsoid, that displays the magnitudes of the mass/inertial properties directly rather than their square roots. Our study of serial macro/mini structures is based on two models of redundant mechanisms. The first is a description of the task-level dynamics that results from projecting the system dynamics into operational space. The second is a unique dynamically consistent relationship between end-effector forces and joint torques. It divides control torques at the joint level into two dynamically decoupled vectors: torques that correspond to forces at the end effector, and torques that affect only internal motions. The analysis of inertial properties of macro-/mini-manipulator systems reveals another important characteristic: that of reduced effective inertia. We show that the effective mass/inertia of a macro-/mini-manipulator is bounded above by the mass/inertia of the mini-manipulator alone. Because mini structures have a limited range of motion, we also propose a dextrous dynamic coordination strategy to allow full use of the high mechanical bandwidth of the mini-structures in extended-motion operations. Finally, a study of the dynamics of parallel, multiarm structures reveals an important additive property. The effective mass and inertia of a multiarm system at some operational point are shown to be given by the sum of the effective masses and inertias associated with the object and each arm. Using this property, the multiarm system can be treated as a single augmented object and controlled by the total operational forces applied by the arms. Both the augmented object construct and the dynamically consistent force/torque relationship are extended for the analysis and control of multiarm systems involving redundancy.

The International Journal of Robotics Research,
Vol. 13, No. 1, February 1995, pp. 19-36.
© 1995 Massachusetts Institute of Technology.

1. Introduction

Dealing with dynamics is essential for achieving higher performance in robotic manipulation. Robot dynamics has been traditionally viewed from the perspective of a manipulator's joint motions, and significant effort has been devoted to the development of *joint-space* dynamic models and control methodologies. However, the limitations of joint-space control techniques, especially in constrained motion tasks, have motivated alternative approaches for dealing with task-level dynamics and control (Takase 1977; Luh, Walker, and Paul 1980; Hogan 1984). The *operational space formulation* (Khatib 1980, 1987), which falls within this line of research, has been driven by the need to develop mathematical models for the description, analysis, and control of robot dynamics with respect to task behavior. In this framework, both motions and active forces are addressed at the same level of end-effector control. The result is a unified approach for dynamic control of end-effector motions and contact forces.

The dynamic performance of a manipulator is strongly dependent on the inertial and acceleration characteristics that are perceived at its end effector. Incorporating lightweight links (i.e., a mini-manipulator) at the end-of-arm can greatly improve these characteristics and significantly increase the ability of the manipulator to perform fine motions (Cai and Roth 1987; Sharon, Hogan, and Hardt 1988). The development of fine-positioning devices has received increased attention in recent years. Micro electromagnetic devices with two and three degrees of freedom (Hollis 1985; Hammer et al. 1992; Karidis et al. 1992) have shown high performance, excellent precision, and speed. Mini-devices have also been used to

Downloaded from ijr.sagepub.com at Bobst Library, New York University on May 9, 2015

provide improved force control capabilities (Reboulet and Robert 1986; Merlet 1988) and increased performance in the control of flexible arms (Tilley et al. 1986).

Clearly, the higher accuracy and greater speed of a mini-manipulator are useful for small motion operations during which the rest of the manipulator can be held motionless. In force control tasks, a mini-manipulator can be used to overcome manipulator errors in the directions of force control by using end-effector force sensing to perform small and fast adjustments. However, the high performance of a mini-manipulator is only available within the mechanically limited range of its joint motions. An effective coordination strategy between the macro and mini structures is therefore essential for extending this performance to tasks covering a wide range of motions (Khatib 1990). This article analyzes the inertial properties of macro-/mini-manipulator systems and presents a general methodology for their coordination and control.

Another area in which dynamics plays a critical role is multiarm robot systems. Multiarm control has generally been treated as a motion coordination problem. One of the first schemes for the control of a two-arm system (Alford and Belyeu 1984) was organized in a master/slave fashion and used a motion coordination procedure to minimize errors in the relative position of the two manipulators. In another study (Zheng and Luh 1986), one manipulator was treated as a "leader" and the other as a "follower." Control of the follower was based on the constraint relationships between the two manipulators. In contrast, the two manipulators were given a symmetric role in the coordination proposed by Uchiyama and Dauchez (1988). The problem of controlling both motion and force in multiarm systems has been investigated by Hayati (1986). In that proposed approach, the load is partitioned among the arms. Dynamic decoupling and motion control are then achieved at the level of individual manipulator effectors. In the force control subspace, the magnitude of forces is minimized. Tarn et al. (1987) developed a closed-chain dynamic model for a two-manipulator system with respect to a selected set of generalized joint coordinates. Nonlinear feedback and output decoupling techniques were then used to linearize and control the system in task coordinates. Linearizing and output decoupling of two-arm systems has also been investigated in Kumar et al. (1991). This article presents the *augmented object* model, which extends the operational space approach to multiarm robot systems.

Sections 2 and 3 review the basics of the operational space framework and discuss its extension to redundant manipulators. The models for the description of inertial properties and the *belted-ellipsoid* representation are presented in Section 4. Section 5 discusses *reduced effective inertia* and *dextrous dynamic coordination* for macro-/mini-manipulator systems. The *augmented object model* and its extension to redundant multiarm robot systems are presented in Sections 6 and 7.

2. Operational Space Dynamics

The inertial properties of a manipulator are generally expressed with respect to its motion in joint space. For an n-degree-of-freedom manipulator, the joint-space inertial properties are described by the $n \times n$ configuration dependent matrix, $\mathbf{A}(\mathbf{q})$, associated with the quadratic form of its kinetic energy, $\frac{1}{2}\,\dot{\mathbf{q}}^T\mathbf{A}(\mathbf{q})\dot{\mathbf{q}}$, where $\mathbf{q}$ and $\dot{\mathbf{q}}$ are the vectors of joint positions and joint velocities, respectively. The joint-space equations of motion may be written

$$\mathbf{A}(\mathbf{q})\ddot{\mathbf{q}} + \mathbf{b}(\mathbf{q}, \dot{\mathbf{q}}) + \mathbf{g}(\mathbf{q}) = \Gamma, \tag{1}$$

where $\mathbf{b}(\mathbf{q}, \dot{\mathbf{q}})$ is the vector of centrifugal and Coriolis joint forces and $\mathbf{g}(\mathbf{q})$ is the gravity joint-force vector. Γ is the vector of generalized joint forces.

When the dynamic response or impact force at some point at the end effector or manipulated object is of interest, the inertial properties involved are those evaluated at that point, termed the *operational point*. Attaching a coordinate frame to the end effector at the operational point and using the relationships between this frame and the reference frame attached to the manipulator base provides a description, $\mathbf{x}$, of the configuration (i.e., position and orientation) of the effector.

The number, m, of independent parameters needed to describe the position and orientation of the end effector determines its number of degrees of freedom. When the effector and manipulator have both the same degree of freedom (i.e., $n = m$), the *operational coordinates*, $\mathbf{x}$, form a set of generalized coordinates for the mechanism (Khatib 1987) in a domain of the workspace that excludes the kinematic singularities. In this case, the kinetic energy of the mechanism is a quadratic form of the generalized operational velocities, $\frac{1}{2}\,\dot{\mathbf{x}}^T\mathbf{\Lambda}(\mathbf{x})\dot{\mathbf{x}}$, where $\mathbf{\Lambda}(\mathbf{x})$ is the $m \times m$ kinetic energy matrix associated with the operational space.

This operational space kinetic energy matrix, $\mathbf{\Lambda}(\mathbf{x})$, provides a description of the inertial properties of the manipulator at the operational point. The relationship between the operational and joint-space matrices, $\mathbf{\Lambda}(\mathbf{x})$ and $\mathbf{A}(\mathbf{q})$, can be established by stating the identity between the two quadratic forms of kinetic energy and by using the relationship between joint velocities and effector velocities, which involves the Jacobian matrix, $\mathbf{J}(\mathbf{q})$. This yields

$$\mathbf{\Lambda}(\mathbf{x}) = \mathbf{J}^{-T}(\mathbf{q})\mathbf{A}(\mathbf{q})\mathbf{J}^{-1}(\mathbf{q}). \tag{2}$$

The matrix $\mathbf{\Lambda}(\mathbf{x})$, along with its partial derivatives with respect to the operational coordinates (coefficients of centrifugal and Coriolis forces), and the gravity forces acting at the operational point establish the equations

Downloaded from ijr.sagepub.com at Bobst Library, New York University on May 9, 2015

of motion (Khatib 1980) for the effector subjected to operational forces, $\mathbf{F}$. These equations are

$$\Lambda(\mathbf{x})\ddot{\mathbf{x}} + \mu(\mathbf{x}, \dot{\mathbf{x}}) + \mathbf{p}(\mathbf{x}) = \mathbf{F}, \tag{3}$$

where $\mu(\mathbf{x}, \dot{\mathbf{x}})$ and $\mathbf{p}(\mathbf{x})$ are, respectively, the centrifugal and Coriolis force vector and the gravity force vector acting in operational space.

2.1. Basic Dynamic Model

By the nature of coordinates associated with spatial rotations, operational forces acting along rotation coordinates are not homogeneous to moments and vary with the type of representation being used (e.g., Euler angles, direction cosines, Euler parameters, quaternions). Although this characteristic does not raise any difficulty in free motion operations, the homogeneity issue is important in tasks where both motions and active forces are involved. This issue is also a concern in the analysis of inertial properties. These properties are expected to be independent of the type of representation used for the description of the end-effector orientation.

The homogeneity issue is addressed by using the relationships between operational velocities and instantaneous angular velocities. The Jacobian matrix $\mathbf{J}(\mathbf{q})$ associated with a given selection, $\mathbf{x}$, of operational coordinates can be expressed (Khatib 1987) as

$$\mathbf{J}(\mathbf{q}) = \mathbf{E}(\mathbf{x})\mathbf{J}_0(\mathbf{q}), \tag{4}$$

where the matrix $\mathbf{J}_0(\mathbf{q})$, termed *the basic Jacobian*, is defined independently of the particular set of parameters used to describe the end-effector configuration, whereas the matrix $\mathbf{E}(\mathbf{x})$ is dependent on those parameters. The basic Jacobian establishes the relationships between generalized joint velocities $\dot{\mathbf{q}}$ and end-effector linear and angular velocities $\mathbf{v}$ and ω.

$$\vartheta \triangleq \begin{bmatrix} \mathbf{v} \\ \omega \end{bmatrix} = \mathbf{J}_0(\mathbf{q})\dot{\mathbf{q}}. \tag{5}$$

Using the basic Jacobian matrix, the mass and inertial properties at the end effector are described by

$$\Lambda_0(\mathbf{x}) = \mathbf{J}_0^{-T}(\mathbf{q})\mathbf{A}(\mathbf{q})\mathbf{J}_0^{-1}(\mathbf{q}). \tag{6}$$

The above matrix is related to the kinetic energy matrix associated with a set of operational coordinates, $\mathbf{x}$, by

$$\Lambda(\mathbf{x}) = \mathbf{E}^{-T}(\mathbf{x})\Lambda_0(\mathbf{x})\mathbf{E}^{-1}(\mathbf{x}). \tag{7}$$

Like angular velocities, moments are defined as instantaneous quantities. A generalized operational force vector, $\mathbf{F}$, associated with a set of operational coordinates, $\mathbf{x}$, is related to forces and moments by

$$\mathbf{F}_0 \triangleq \begin{bmatrix} \mathcal{F} \\ \mathcal{M} \end{bmatrix} = \mathbf{E}^T(\mathbf{x})\ \mathbf{F}, \tag{8}$$

where $\mathcal{F}$ and $\mathcal{M}$ are the vectors of forces and moments. With respect to linear and angular velocities, the end-effector equation of motion can be written as

$$\Lambda_0(\mathbf{x})\dot{\vartheta} + \mu_0(\mathbf{x}, \vartheta) + \mathbf{p}_0(\mathbf{x}) = \mathbf{F}_0, \tag{9}$$

where $\Lambda_0(\mathbf{x})$, $\mu_0(\mathbf{x}, \vartheta)$, and $\mathbf{p}_0(\mathbf{x})$ are defined similarly to $\Lambda(\mathbf{x})$, $\mu(\mathbf{x}, \dot{\mathbf{x}})$, and $\mathbf{p}(\mathbf{x})$ using $\mathbf{J}_0(\mathbf{q})$ instead of $\mathbf{J}(\mathbf{q})$. With equation (9), the dynamics of the end effector is described with respect to linear and angular velocities. Therefore, a task transformation of the description of end-effector orientation is needed. Such a transformation involves the inverse of $\mathbf{E}(\mathbf{x})$ and its derivatives (Khatib 1980).

2.2. Unified Motion and Force Control

Equation (9) is the basis for the development of the unified framework for motion and force control. Compliant motion and part mating operations involve motion control in some directions and force control in orthogonal directions, as illustrated in Figure 1. Such tasks are described by the *generalized selection matrix* Ω and its complement $\overline{\Omega}$ associated with motion control and force control, respectively (Khatib 1987). Using equation (9), the end-effector/sensor equations of motion can be written as

$$\Lambda_0(\mathbf{x})\dot{\vartheta} + \mu_0(\mathbf{x}, \vartheta) + \mathbf{p}_0(\mathbf{x}) + \mathbf{F}_{\text{contact}} = \mathbf{F}_0. \tag{10}$$

The vector $\mathbf{F}_{\text{contact}}$ represents the contact forces acting at the end effector. The unified approach for end-effector dynamic decoupling, motion, and active force control is achieved by selecting the control structure

$$\mathbf{F}_0 = \mathbf{F}_{\text{motion}} + \mathbf{F}_{\text{active-force}}, \tag{11}$$

where

$$\mathbf{F}_{\text{motion}} = \widehat{\Lambda}_0(\mathbf{x})\Omega\mathbf{F}^*_{\text{motion}} + \widehat{\mu}_0(\mathbf{x}, \vartheta) + \widehat{\mathbf{p}}_0(\mathbf{x}), \tag{12}$$

$$\mathbf{F}_{\text{active-force}} = \widehat{\Lambda}_0(\mathbf{x})\overline{\Omega}\mathbf{F}^*_{\text{active-force}} + \mathbf{F}_{\text{sensor}}, \tag{13}$$

and $\widehat{\Lambda}_0(\mathbf{x})$, $\widehat{\mu}_0(\mathbf{x}, \dot{\mathbf{x}})$, and $\widehat{\mathbf{p}}_0(\mathbf{x})$ represent the estimates of $\Lambda_0(\mathbf{x})$, $\mu_0(\mathbf{x}, \dot{\mathbf{x}})$, and $\mathbf{p}_0(\mathbf{x})$. The vectors $\mathbf{F}^*_{\text{motion}}$ and

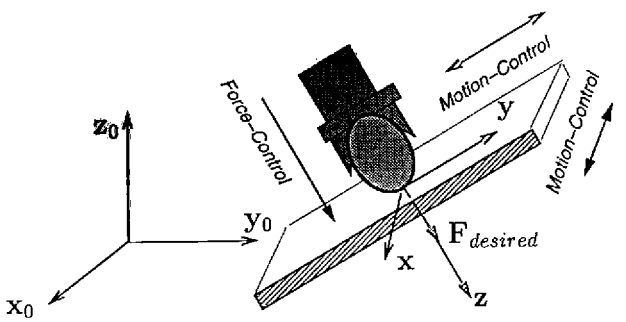

Fig. 1. A constrained motion task.

Downloaded from ijr.sagepub.com at Bobst Library, New York University on May 9, 2015

$\mathbf{F}^{\star}_{\text{active}-\text{force}}$ represent the inputs to the decoupled system. The generalized joint forces $\boldsymbol{\Gamma}$ required to produce the operational forces $\mathbf{F}_0$ are

$$\boldsymbol{\Gamma} = \mathbf{J}_0^T(\mathbf{q})\mathbf{F}_0. \tag{14}$$

With perfect estimates of the dynamic parameters and perfect sensing of contact forces (i.e., $\mathbf{F}_{\text{sensor}} = \mathbf{F}_{\text{contact}}$), the closed loop system is described by the following two decoupled subsystems:

$$\boldsymbol{\Omega}\dot{\boldsymbol{\vartheta}} = \boldsymbol{\Omega}\mathbf{F}^{\star}_{\text{motion}}, \tag{15}$$

$$\overline{\boldsymbol{\Omega}}\dot{\boldsymbol{\vartheta}} = \overline{\boldsymbol{\Omega}}\mathbf{F}^{\star}_{\text{active}-\text{force}}. \tag{16}$$

The unified motion and force control system is shown in Figure 2.

3. Redundancy in Manipulation

A manipulator is said to be *redundant* when the number, n, of its degrees of freedom is greater than the number, m, of its end-effector degrees of freedom. In this definition, redundancy is a characteristic of the manipulator. The extent of the manipulator redundancy is given by $(n - m)$, which defines the manipulator degree of redundancy.

In manipulation there is also *task redundancy*. This type of redundancy is associated with tasks that involve a subset of the parameters needed to describe the configuration of the end effector. This redundancy concerns all types of manipulators. For instance, positioning the end effector of a nonredundant manipulator results in a *redundancy with respect to the task* of controlling the end-effector position.

A manipulator is said to be redundant with respect to a task if the number, m_{Task}, of independent parameters needed to describe the task configuration is smaller than the number n of the manipulator degrees of freedom.

3.1. Dynamics of Redundant Manipulators

A set of operational coordinates describing only the end-effector position and orientation is obviously insufficient to completely specify the configuration of a redundant manipulator. Therefore, the dynamic behavior of the entire system cannot be described by a dynamic model using operational coordinates. Nevertheless, the dynamic behavior of the end effector itself can still be described, and its equations of motion in operational space can still be established. In fact, the structure of the effector dynamic model has been shown (Khatib 1980, 1987) to be identical to that obtained in the case of nonredundant manipulators (equation (3)). In the redundant case, however, the matrix $\boldsymbol{\Lambda}$ should be interpreted as a "*pseudo kinetic energy matrix*." As shown below, this matrix is related to the joint-space kinetic energy matrix by

$$\boldsymbol{\Lambda}^{-1}(\mathbf{q}) = \mathbf{J}(\mathbf{q})\mathbf{A}^{-1}(\mathbf{q})\mathbf{J}^T(\mathbf{q}). \tag{17}$$

The above relationship provides a general expression for the matrix $\boldsymbol{\Lambda}$ that applies to both redundant and nonredundant manipulators. Although equation (3) provides a description of the whole system dynamics for nonredundant manipulators, the equation associated with a redundant manipulator only describes the dynamic behavior of its end effector. In that case, the equation can be thought of as a "*projection*" of the system's dynamics into the operational space. The remainder of the dynamics will affect joint motions in the null space of the redundant system. This analysis is discussed below.

The operational space equations of motion describe the dynamic response of a manipulator to the application of an operational force $\mathbf{F}$ at the end effector. For nonredundant manipulators, the relationship between operational forces, $\mathbf{F}$, and joint torques, $\boldsymbol{\Gamma}$, is

$$\boldsymbol{\Gamma} = \mathbf{J}^T(\mathbf{q})\mathbf{F}. \tag{18}$$

However, this relationship becomes incomplete for redundant manipulators that are in motion. Analysis of the kinematic aspect of redundancy shows that, at a given configuration, there is an infinity of elementary displacements of the redundant mechanism that could take place without altering the configuration of the effector. Those displacements correspond to motion in the null space associated with a generalized inverse of the Jacobian matrix.

There is also a null space associated with some inverse of the transpose of the Jacobian matrix. When the redundant manipulator is not at static equilibrium, there is an infinity of joint torque vectors that could be applied without affecting the resulting forces at the end effector. These are the joint torques acting within the null space. With the addition of null space joint torques, the relationship between end-effector forces and manipulator joint torques takes the following general form:

$$\boldsymbol{\Gamma} = \mathbf{J}^T(\mathbf{q})\mathbf{F} + \left[\mathbf{I} - \mathbf{J}^T(\mathbf{q})\mathbf{J}^{T^{\#}}(\mathbf{q})\right]\boldsymbol{\Gamma}_0, \tag{19}$$

where $\boldsymbol{\Gamma}_0$ is an arbitrary generalized joint torque vector, which will be projected in the null space of $\mathbf{J}^{T^{\#}}$, and $\mathbf{J}^{T^{\#}}$ is a generalized inverse of $\mathbf{J}^T$. Clearly, equation (19) is dependent on $\mathbf{J}^{T^{\#}}$, and there is an infinity of generalized inverses for $\mathbf{J}^T$: namely, $\{\mathbf{J}^{T^{\#}} \mid \mathbf{J}^T = \mathbf{J}^T\mathbf{J}^{T^{\#}}\mathbf{J}^T\}$. Below, it is shown that only one of these generalized inverses is consistent with the system dynamics.

We start by applying to the manipulator system (1), a joint torque vector in the general form (19). To establish the relationship between operational acceleration and

Downloaded from ijr.sagepub.com at Bobst Library, New York University on May 9, 2015

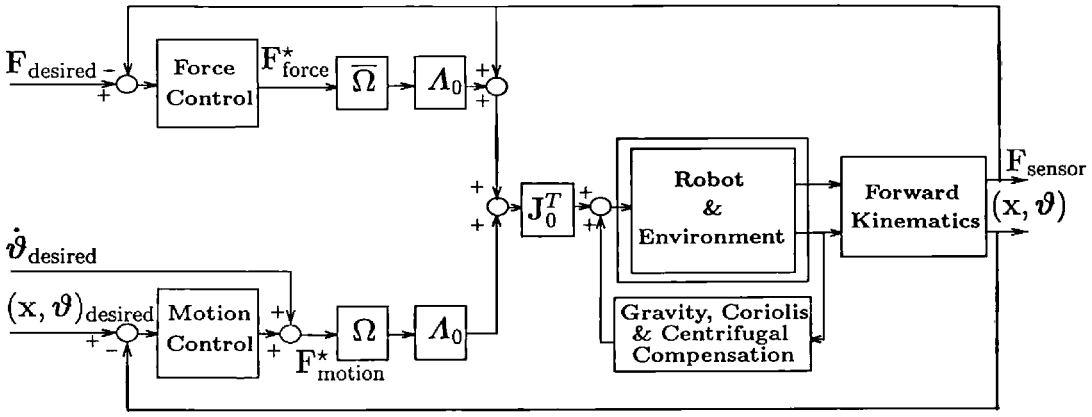

Fig. 2. Unified motion and force control structure.

operational force, we premultiply equation (1) by the matrix $\mathbf{J}(\mathbf{q})\mathbf{A}^{-1}(\mathbf{q})$ and use the relationship between joint acceleration and operational accelerations ($\ddot{\mathbf{x}} - \dot{\mathbf{J}}(\mathbf{q})\dot{\mathbf{q}} = \mathbf{J}(\mathbf{q})\ddot{\mathbf{q}}$). The resulting equation can be written as

$$\begin{aligned}\ddot{\mathbf{x}} &+ \left(\mathbf{J}(\mathbf{q})\mathbf{A}^{-1}(\mathbf{q})\mathbf{b}(\mathbf{q},\dot{\mathbf{q}}) - \dot{\mathbf{J}}(\mathbf{q})\dot{\mathbf{q}}\right) \\ &+ \mathbf{J}(\mathbf{q})\mathbf{A}^{-1}(\mathbf{q})\mathbf{g}(\mathbf{q}) = \left(\mathbf{J}(\mathbf{q})A^{-1}(\mathbf{q})\mathbf{J}^{T}(\mathbf{q})\right)\mathbf{F} \\ &+ \mathbf{J}(\mathbf{q})\mathbf{A}^{-1}(\mathbf{q})\left[\mathbf{I} - \mathbf{J}^{T}(\mathbf{q})\mathbf{J}^{T^{\#}}(\mathbf{q})\right]\Gamma_0. \qquad (20)\end{aligned}$$

This equation expresses the relationship between $\ddot{\mathbf{x}}$ and $\mathbf{F}$. The matrix $\left(\mathbf{J}(\mathbf{q})\mathbf{A}^{-1}(\mathbf{q})\mathbf{J}^{T}(\mathbf{q})\right)$, which premultiplies $\mathbf{F}$, is homogeneous to the inverse of a kinetic energy matrix. This matrix, which exists everywhere outside kinematic singularities, is the *pseudo kinetic energy matrix* of equation (17)

$$\mathbf{\Lambda}(\mathbf{q}) = \left(\mathbf{J}(\mathbf{q})\mathbf{A}^{-1}(\mathbf{q})\mathbf{J}^{T}(\mathbf{q})\right)^{-1}.$$

Equation (20) shows that the acceleration at the operational point is affected by Γ_0 unless the term involving Γ_0 is zero. That is, for joint torques associated with the null space in equation (19) not to produce any operational acceleration, it is necessary that

$$\mathbf{J}(\mathbf{q})\mathbf{A}^{-1}(\mathbf{q})\left[\mathbf{I} - \mathbf{J}^{T}(\mathbf{q})\mathbf{J}^{\#^{T}}(\mathbf{q})\right]\Gamma_0 = 0. \qquad (21)$$

A generalized inverse of $J(\mathbf{q})$ satisfying the above constraint is said to be *dynamically consistent* (Khatib 1990).

THEOREM 1. DYNAMIC CONSISTENCY. A generalized inverse that is consistent with the dynamic constraint of equation (21), $\bar{\mathbf{J}}(\mathbf{q})$, is unique and is given by

$$\bar{\mathbf{J}}(\mathbf{q}) = \mathbf{A}^{-1}(\mathbf{q})\mathbf{J}^{T}(\mathbf{q})\mathbf{\Lambda}(\mathbf{q}). \qquad (22)$$

The proof is based on a straightforward analysis of equation (21). This equation can be rewritten as

$$\left[\mathbf{J}(\mathbf{q})\mathbf{A}^{-1}(\mathbf{q}) - \left(\mathbf{J}(\mathbf{q})\mathbf{A}^{-1}(\mathbf{q})\mathbf{J}^{T}(\mathbf{q})\right)\mathbf{J}^{\#^{T}}(\mathbf{q})\right]\Gamma_0 = 0,$$

which, using the definition of $\mathbf{\Lambda}$, yields

$$\mathbf{\Lambda}(\mathbf{q})\mathbf{J}(\mathbf{q})\mathbf{A}^{-1}(\mathbf{q}) = \mathbf{J}^{\#^{T}}(\mathbf{q}).$$

Notice that $\bar{\mathbf{J}}(\mathbf{q})$ of equation (22) is actually the generalized inverse of the Jacobian matrix corresponding to the solution of $\delta\mathbf{x} = \mathbf{J}(\mathbf{q})\delta\mathbf{q}$ that minimizes the manipulator's instantaneous kinetic energy.

3.1.1. *Equations of Motion of Redundant Manipulators*

The end-effector equations of motion for a redundant manipulator can be obtained by using the dynamically consistent generalized inverse in equation (20) and premultiplying this equation by the matrix $\mathbf{\Lambda}(\mathbf{q})$. The resulting equations are of the same form as equation (3) established for nonredundant manipulators. In the case of redundancy, however, the inertial properties vary not only with the end-effector configuration, but also with the manipulator posture.

$$\mathbf{\Lambda}(\mathbf{q})\ddot{\mathbf{x}} + \mu(\mathbf{q},\dot{\mathbf{q}}) + \mathbf{p}(\mathbf{q}) = \mathbf{F}, \qquad (23)$$

where

$$\mu(\mathbf{q},\dot{\mathbf{q}}) = \bar{\mathbf{J}}^{T}(\mathbf{q})\mathbf{b}(\mathbf{q},\dot{\mathbf{q}}) - \mathbf{\Lambda}(\mathbf{q})\dot{\mathbf{J}}(\mathbf{q})\dot{\mathbf{q}}, \qquad (24)$$

$$\mathbf{p}(\mathbf{q}) = \bar{\mathbf{J}}^{T}(\mathbf{q})\mathbf{g}(\mathbf{q}). \qquad (25)$$

Equation (23) provides a description of the dynamic behavior of the end effector in operational space. This equation is simply the projection of the joint-space equations of motion (1), by the dynamically consistent generalized inverse $\bar{\mathbf{J}}^{T}(\mathbf{q})$,

$$\begin{aligned}\bar{\mathbf{J}}^{T}(\mathbf{q})\ \{\mathbf{A}(\mathbf{q})\ddot{\mathbf{q}} + \mathbf{b}(\mathbf{q},\dot{\mathbf{q}}) + \mathbf{g}(\mathbf{q}) = \Gamma\} \qquad (26)\\ \Longrightarrow \quad \mathbf{\Lambda}(\mathbf{q})\ddot{\mathbf{x}} + \mu(\mathbf{q},\dot{\mathbf{q}}) + \mathbf{p}(\mathbf{q}) = \mathbf{F}.\end{aligned}$$

The above property also applies to nonredundant manipulators, where the matrix $\bar{\mathbf{J}}^{T}(\mathbf{q})$ reduces to $\mathbf{J}^{-T}(\mathbf{q})$.

Downloaded from ijr.sagepub.com at Bobst Library, New York University on May 9, 2015

3.1.2. Dynamically Consistent Torque-Force Relationship

The dynamically consistent relationship between joint torques and operational forces for redundant manipulator systems is

$$\Gamma = \mathbf{J}^T(\mathbf{q})\mathbf{F} + \left[\mathbf{I} - \mathbf{J}^T(\mathbf{q})\bar{\mathbf{J}}^T(\mathbf{q})\right]\Gamma_0. \qquad (27)$$

This relationship provides a decomposition of joint torques into two dynamically decoupled control vectors: joint torques corresponding to forces acting at the end effector ($\mathbf{J}^T\mathbf{F}$); and joint torques that only affect internal motions, $\left([\mathbf{I} - \mathbf{J}^T(\mathbf{q})\bar{\mathbf{J}}^T(\mathbf{q})]\Gamma_0\right)$.

Using this decomposition, the end effector can be controlled by operational forces, whereas internal motions can be independently controlled by joint torques that are guaranteed not to alter the end effector's dynamic behavior. This relationship is the basis for implementing the dextrous dynamic coordination strategy for macro-/mini-manipulators to be discussed in Section 5.3.

4. Inertial Properties

The analysis of the end-effector inertial properties relies on study of the matrix

$$\mathbf{\Lambda}_0(\mathbf{q}) = \left(\mathbf{J}_0(\mathbf{q})\mathbf{A}^{-1}(\mathbf{q})\mathbf{J}_0^T(\mathbf{q})\right)^{-1},$$

where $\mathbf{J}_0(\mathbf{q})$ is the basic Jacobian associated with the end-effector linear and angular velocities. Using this matrix, Asada (1983) proposed the generalized inertia ellipsoid as a geometric representation for the inertial properties of a manipulator. An alternative to the ellipsoid of inertia is the ellipsoid of gyration suggested by Hogan (1984). This ellipsoid is based on analysis of the matrix, $\mathbf{\Lambda}_0^{-1}(\mathbf{q})$, whose existence is always guaranteed. The eigenvalues and eigenvectors of the matrix $\mathbf{\Lambda}_0(\mathbf{q})$ were used in combination with the hyper-parallelepiped of acceleration in the design of manipulators aimed at achieving the smallest, most isotropic, and most uniform inertial characteristics; and the largest, most isotropic, and most uniform bounds on the magnitude of end-effector acceleration (Khatib and Burdick 1985, Khatib and Agrawal 1989).

The eigenvalues associated with the matrix $\mathbf{\Lambda}_0(\mathbf{q})$ or its inverse $\mathbf{\Lambda}_0^{-1}(\mathbf{q})$ provide a useful characterization of the bounds on the magnitude of the inertial properties. However, these eigenvalues correspond to eigenvectors in a six-dimensional space that combines translational and rotational motions and are difficult to interpret.

4.1. Inertial Properties and Task Redundancy

When analyzing the inertial properties of manipulators, two distinct types of tasks are examined: end-effector translational tasks and end-effector rotational tasks. Given the redundancy of the manipulator with respect to each of these tasks, the dynamic behavior at the end-effector can be described by a system of equations similar to (23).

First, let us consider the task of positioning the end effector. The Jacobian in this case is the matrix, $\mathbf{J}_v(\mathbf{q})$, associated with the linear velocity at the operational point. The pseudo kinetic energy matrix is:

$$\mathbf{\Lambda}_v^{-1}(\mathbf{q}) = \mathbf{J}_v(\mathbf{q})\mathbf{A}^{-1}(\mathbf{q})\mathbf{J}_v^T(\mathbf{q}). \qquad (28)$$

The matrix $\mathbf{\Lambda}_v^{-1}(\mathbf{q})$ provides a description of the end-effector translational response to a force. Consider, for instance, the task of positioning the end effector along the y-axis, as illustrated in Figure 3*A*. The Jacobian associated with this task reduces to the row matrix $\mathbf{J}_{v_y}(\mathbf{q})$. The pseudo kinetic energy matrix in this case is a scalar, m_y, representing the mass perceived at the end effector in response to the application of a force f_y along the y-axis:

$$\frac{1}{m_y} = \mathbf{J}_{v_y}(\mathbf{q})\mathbf{A}^{-1}(\mathbf{q})\mathbf{J}_{v_y}^T(\mathbf{q}).$$

With $\mathbf{y}_0$ representing the unit vector along the y-axis, the matrix $\mathbf{J}_{v_y}(\mathbf{q})$ can be written as

$$\mathbf{J}_{v_y}(\mathbf{q}) = \mathbf{y}_0^T\mathbf{J}_v(\mathbf{q}),$$

and

$$\frac{1}{m_y} = \mathbf{y}_0^T\mathbf{\Lambda}_v^{-1}\mathbf{y}_0.$$

For rotational tasks, the Jacobian involved is the matrix $\mathbf{J}_\omega(\mathbf{q})$ associated with the angular velocity measured about the different axes of the operational frame. The pseudo kinetic energy matrix

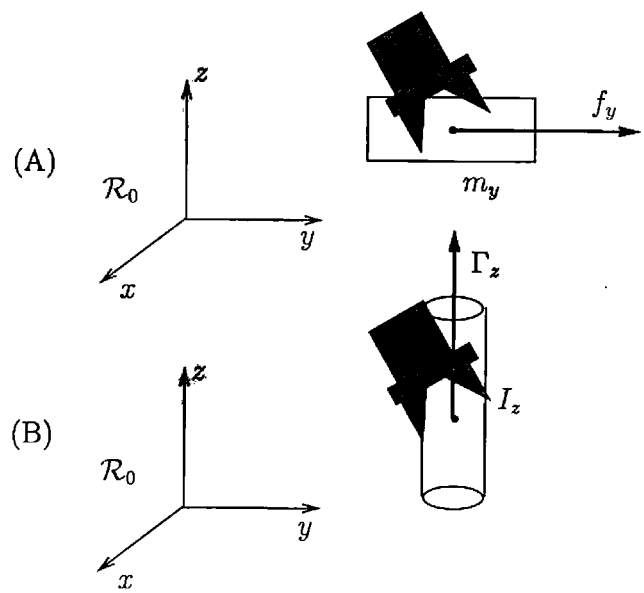

Fig. 3. Effective mass (A) and effective inertia (B).

Downloaded from ijr.sagepub.com at Bobst Library, New York University on May 9, 2015

is:

$$\Lambda_{\omega}^{-1}(\mathbf{q}) = \mathbf{J}_{\omega}(\mathbf{q})\mathbf{A}^{-1}(\mathbf{q})\mathbf{J}_{\omega}^{T}(\mathbf{q}). \tag{29}$$

The matrix $\Lambda_{\omega}^{-1}(\mathbf{q})$ provides a description of the end-effector rotational response to a moment. Consider now the task of rotating the end effector about the z-axis, as illustrated in Figure 3*B*. The Jacobian associated with this task is the row matrix

$$\mathbf{J}_{\omega_z}(\mathbf{q}) = \mathbf{z}_0^T\mathbf{J}_{\omega}(\mathbf{q}).$$

$\mathbf{z}_0$ is the unit vector along the z-axis. The pseudo kinetic energy matrix in this case is a scalar, $\mathbf{I}_z$, representing the inertia perceived at the end effector in response to a moment Γ_z applied about the z-axis:

$$\frac{1}{\mathbf{I}_z} = \mathbf{z}_0^T\Lambda_{\omega}^{-1}(\mathbf{q})\mathbf{z}_0.$$

4.2. *Effective Mass/Inertia*

The above analysis can be easily extended for translational and rotational motions along or about an arbitrary direction. If $\mathbf{u}$ is the unit vector describing this direction, the inertial properties can be analyzed by considering the two matrices $\mathbf{J}_{v_u}(\mathbf{q})$ and $\mathbf{J}_{\omega_u}(\mathbf{q})$. These matrices are given by

$$\mathbf{J}_{v_u}(\mathbf{q}) = \mathbf{u}^T\mathbf{J}_v(\mathbf{q}) \quad \text{and} \quad \mathbf{J}_{\omega_u}(\mathbf{q}) = \mathbf{u}^T\mathbf{J}_{\omega}(\mathbf{q}).$$

The *effective mass*, $m_{\mathbf{u}}(\Lambda_v)$, perceived at the operational point along a direction $\mathbf{u}$ is given by

$$\frac{1}{m_{\mathbf{u}}(\Lambda_v)} = \mathbf{u}^T\Lambda_v^{-1}(\mathbf{q})\mathbf{u}. \tag{30}$$

Starting from rest, the inverse of magnitude of the effective mass is equal to the component of the linear acceleration along the direction $\mathbf{u}$ that results in response to a unit force applied along $\mathbf{u}$.

The *effective inertia*, $I_{\mathbf{u}}(\Lambda_{\omega})$, perceived at the operational point about a direction $\mathbf{u}$ is given by

$$\frac{1}{I_{\mathbf{u}}(\Lambda_{\omega})} = \mathbf{u}^T\Lambda_{\omega}^{-1}(\mathbf{q})\mathbf{u}. \tag{31}$$

Starting from rest, the inverse of magnitude of the effective inertia is equal to the component of the angular acceleration about the direction $\mathbf{u}$ that results in response to a unit moment applied about $\mathbf{u}$.

4.3. *Structure of* Λ_0^{-1}

We have seen that the end-effector translational response to a force and its rotational response to a moment can be characterized by the matrices $\Lambda_v^{-1}(\mathbf{q})$ and $\Lambda_{\omega}^{-1}(\mathbf{q})$, respectively. These two matrices have been established separately by considering pure translational motion tasks and pure rotational motion tasks.

Consider again the matrix $\left(\mathbf{J}_0(\mathbf{q})\mathbf{A}^{-1}(\mathbf{q})\mathbf{J}_0^T(\mathbf{q})\right)$ expressed in terms of the matrix $\mathbf{A}^{-1}(\mathbf{q})$ and the basic Jacobian $\mathbf{J}_0(\mathbf{q})$. The basic Jacobian matrix can be written as

$$\mathbf{J}_0(\mathbf{q}) = \begin{bmatrix} \mathbf{J}_v(\mathbf{q}) \\ \mathbf{J}_{\omega}(\mathbf{q}) \end{bmatrix}, \tag{32}$$

where $\mathbf{J}_v(\mathbf{q})$ and $\mathbf{J}_{\omega}(\mathbf{q})$ are the two block matrices associated with the end-effector linear and angular velocities, respectively. Using this decomposition, the matrix $\Lambda_0^{-1}(\mathbf{q})$ can be written in the form

$$\Lambda_0^{-1}(\mathbf{q}) = \begin{bmatrix} \Lambda_v^{-1}(\mathbf{q}) & \overline{\Lambda}_{v\omega}(\mathbf{q}) \\ \overline{\Lambda}_{v\omega}^T(\mathbf{q}) & \Lambda_{\omega}^{-1}(\mathbf{q}) \end{bmatrix}, \tag{33}$$

where $\Lambda_v(\mathbf{q})$ is the matrix given in equation (28) and $\Lambda_{\omega}(\mathbf{q})$ is the matrix given in equation (29). The matrix $\overline{\Lambda}_{v\omega}(\mathbf{q})$ is given by

$$\overline{\Lambda}_{v\omega}(\mathbf{q}) = \mathbf{J}_v(\mathbf{q})\mathbf{A}^{-1}(\mathbf{q})\mathbf{J}_{\omega}^T(\mathbf{q}).$$

The matrix $\Lambda_v(\mathbf{q})$, which describes the end-effector translational response to a force, is homogeneous to a mass matrix, while $\Lambda_{\omega}(\mathbf{q})$, which describes the end-effector rotational response to a moment, is homogeneous to an inertia matrix. The matrix $\overline{\Lambda}_{v\omega}(\mathbf{q})$ provides a description of the coupling between translational and rotational motions.

4.4. *Belted Ellipsoid*

As illustrated in Figure 4, one possible representation of the mass/inertial properties associated with the two matrices $\Lambda_v^{-1}(\mathbf{q})$ and $\Lambda_{\omega}^{-1}(\mathbf{q})$ is to use the two ellipsoids:

$$\mathbf{v}^T\Lambda_v^{-1}(\mathbf{q})\mathbf{v} = 1 \quad \text{and} \quad \mathbf{v}^T\Lambda_{\omega}^{-1}(\mathbf{q})\mathbf{v} = 1.$$

However, ellipsoid representations only provide a description of the square roots of effective mass (inertia) in (about) a direction.

We propose a geometric representation that characterizes the actual magnitude of these properties. This representation is based on what we have termed the *belted ellipsoid*. A belted ellipsoid is obtained by a polar transformation of an ellipsoid. A point on the ellipsoid surface is transformed to a point located along the same polar line at a distance equal to the square of the initial point distance. This construction is illustrated in Figure 5.

A point on the ellipsoid represented by a vector $\mathbf{v}$ is transformed into a point on the belted ellipsoid represented by a vector $\mathbf{w}$. The vector $\mathbf{w}$ is collinear to $\mathbf{v}$ and is of a magnitude equal to $\mathbf{v}^T\mathbf{v}$. That is,

$$\mathbf{w} = \|\mathbf{v}\|\mathbf{v}.$$

Downloaded from ijr.sagepub.com at Bobst Library, New York University on May 9, 2015

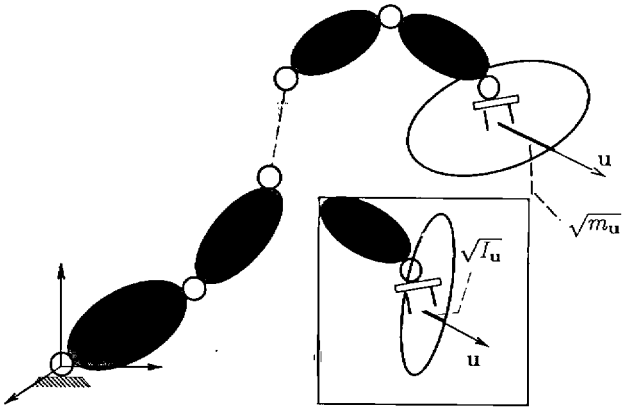

Fig. 4. Effective mass/inertia (ellipsoid representation).

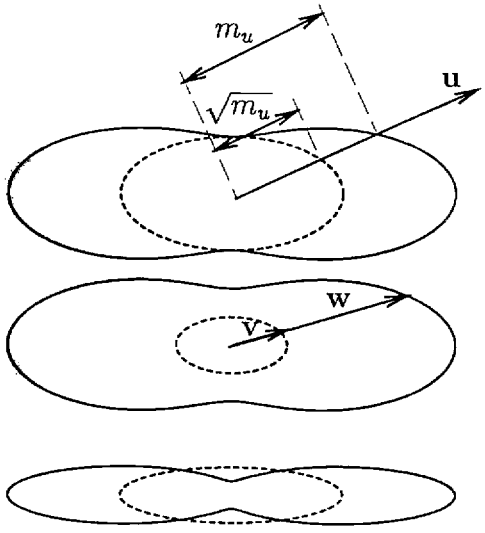

Fig. 5. Construction of belted ellipsoids from ellipsoids.

The equation of a belted ellipsoid, therefore, can be obtained from the equation of an ellipsoid by replacing the vector $\mathbf{v}$ by the vector

$$\frac{\mathbf{v}}{\sqrt{\mathbf{v}^T\mathbf{v}}}.$$

The equations for the two belted ellipsoids corresponding to the two matrices $\mathbf{\Lambda}_v^{-1}(\mathbf{q})$ and $\mathbf{\Lambda}_\omega^{-1}(\mathbf{q})$ are

$$\frac{\mathbf{v}^T\mathbf{\Lambda}_v^{-1}(\mathbf{q})\mathbf{v}}{\sqrt{\mathbf{v}^T\mathbf{v}}} = 1 \quad \text{and} \quad \frac{\mathbf{v}^T\mathbf{\Lambda}_\omega^{-1}(\mathbf{q})\mathbf{v}}{\sqrt{\mathbf{v}^T\mathbf{v}}} = 1. \qquad (34)$$

For instance, the ellipsoid

$$\frac{x^2}{a^2} + \frac{y^2}{b^2} + \frac{z^2}{c^2} = 1$$

becomes

$$\frac{x^2}{a^2\sqrt{x^2+y^2+z^2}} + \frac{y^2}{b^2\sqrt{x^2+y^2+z^2}} + \frac{z^2}{c^2\sqrt{x^2+y^2+z^2}} = 1.$$

Two examples of belted ellipsoids are shown in Figure 6.

For a redundant manipulator, the inertial properties perceived at a given position and orientation of the end effector vary with the manipulator configuration. This is illustrated for the effective mass in Figure 7 using belted ellipsoids.

5. Macro-/Mini-manipulator Systems

Pursuing the investigation of inertial characteristics, we now consider the case of systems resulting from the serial combination of two manipulators. The manipulator connected to the ground will be referred to as the *macro-manipulator*. It has n_M degrees of freedom, and its configuration is described by the system of n_M generalized joint coordinates $\mathbf{q}_M$. The second manipulator, referred to as the *mini-manipulator*, has n_m degrees of freedom and its configuration is described by the generalized coordinates $\mathbf{q}_m$. The resulting structure is an n-degree-of-freedom manipulator with $n = n_M + n_m$. Its configuration is described by the system of generalized joint coordinates $\mathbf{q} = \left[\mathbf{q}_M^T\ \mathbf{q}_m^T\right]^T$. If m represents the number of effector degrees of freedom of the combined structure, n_M and n_m are assumed to obey

$$n_M \geq 1 \quad \text{and} \quad n_m = m. \qquad (35)$$

This assumption says that the mini-manipulator must have the full freedom to move in the operational space.

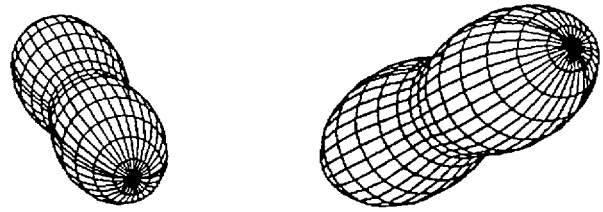

Fig. 6. Examples of belted ellipsoids.

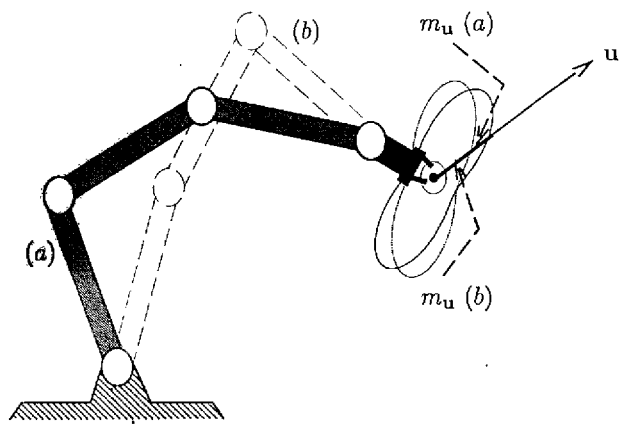

Fig. 7. Effective mass of a redundant manipulator.

Downloaded from ijr.sagepub.com at Bobst Library, New York University on May 9, 2015

The macro-manipulator must have at least one degree of freedom.

5.1. *Kinematics of Macro/Mini Structures*

The configuration of the macro-manipulator is described with respect to a reference frame $\mathcal{R}_0$ and the configuration of the mini-manipulator structure is described with respect to a frame $\mathcal{R}_M$ attached to the last link of the macro-manipulator, as illustrated in Figure 8. The coordinate frame associated with the operational point is denoted by $\mathcal{R}_\odot$. Let $\mathbf{S}_M(\mathbf{q}_M)$ be the transformation matrix describing the rotation between the frames $\mathcal{R}_M$ and $\mathcal{R}_0$.

Let $\mathbf{p}_M$ be the vector connecting the origins of frames $\mathcal{R}_0$ and $\mathcal{R}_M$, and $\mathbf{p}_m$ the vector connecting those of $\mathcal{R}_M$ and $\mathcal{R}_\odot$. The position of the operational point, with respect to $\mathcal{R}_0$, is described by the vector

$$\mathbf{p} = \mathbf{p}_M + \mathbf{p}_m.$$

If $\mathbf{v}_M$ and $\boldsymbol{\omega}_M$ represent the linear and angular velocities at the origin of frame $\mathcal{R}_M$ attached to the last link of the macro-manipulator, the linear velocity at the operational point is

$$\mathbf{v} = \mathbf{v}_M + \mathbf{v}_m + \boldsymbol{\omega}_M \times \mathbf{p}_m,$$

where $\mathbf{v}_m$ represents the linear velocity at the operational point resulting from the motion of the mini-manipulator.

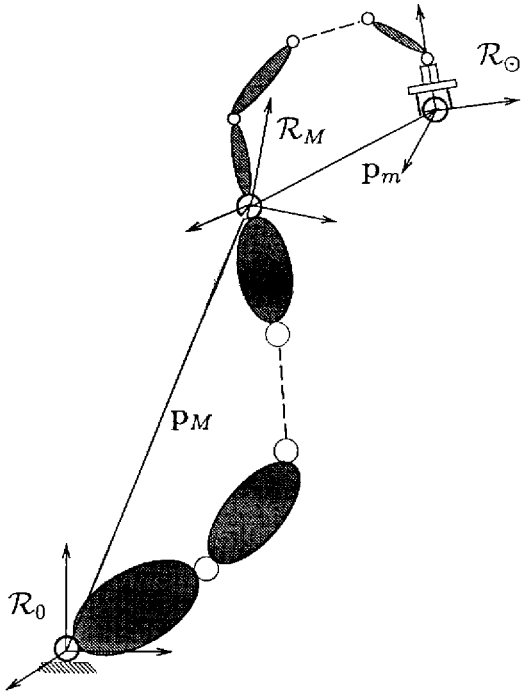

Fig. 8. Kinematics of a macro-/mini-manipulator system.

The angular velocity at the end effector is

$$\boldsymbol{\omega} = \boldsymbol{\omega}_M + \boldsymbol{\omega}_m.$$

Thus, the linear and angular velocities at the operational point expressed with respect to the reference frame $\mathcal{R}_0$ are

$$\begin{bmatrix} \mathbf{v} \\ \boldsymbol{\omega} \end{bmatrix}_{(\mathcal{R}_0)} = \begin{bmatrix} \mathbf{I} & -\widehat{\mathbf{p}}_{m(0)} \\ \mathbf{0} & \mathbf{I} \end{bmatrix} \begin{bmatrix} \mathbf{v}_M \\ \boldsymbol{\omega}_\mathbf{M} \end{bmatrix}_{(\mathcal{R}_0)} + \begin{bmatrix} \mathbf{S}_M & \mathbf{0} \\ \mathbf{0} & \mathbf{S}_M \end{bmatrix} \begin{bmatrix} \mathbf{v}_m \\ \boldsymbol{\omega}_\mathbf{m} \end{bmatrix}_{(\mathcal{R}_M)}, \tag{36}$$

where $\widehat{\mathbf{p}}_{m(0)}$ is the cross-product operator associated with the position vector $\mathbf{p}_{m(0)}$ and expressed in $\mathcal{R}_0$. If $\mathbf{J}_{M(0)}(\mathbf{q}_M)$ and $\mathbf{J}_{m(0)}(\mathbf{q}_m)$ are the basic Jacobian matrices associated with two individual manipulators, the basic Jacobian matrix associated with the serial combination can be expressed as

$$\mathbf{J}_0 = [\, \mathbf{V}\mathbf{J}_{M(0)} \quad \mathbf{J}_{m(0)} \,], \tag{37}$$

where

$$\mathbf{V} = \begin{bmatrix} \mathbf{I} & -\widehat{\mathbf{p}}_{m(0)} \\ \mathbf{0} & \mathbf{I} \end{bmatrix}. \tag{38}$$

5.2. *Dynamics of Macro/Mini Structures*

The kinetic energy matrix, $\mathbf{A}(\mathbf{q})$, of the combined system can be decomposed in block matrices corresponding to the dimensions of the two manipulators' individual kinetic energy matrices

$$\mathbf{A}(\mathbf{q}) = \begin{bmatrix} \mathbf{A}_{11} & \mathbf{A}_{12} \\ \mathbf{A}_{12}^T & \mathbf{A}_{22} \end{bmatrix}. \tag{39}$$

LEMMA 1. The $n_m \times n_m$ joint-space kinetic energy matrix, $\mathbf{A}_m$, of the mini-manipulator considered alone is identical to the matrix $\mathbf{A}_{22}$ of (39).

Proof. The kinetic energy of the combined macro-/mini-manipulator is

$$\mathbf{T}(\mathbf{q}, \dot{\mathbf{q}}) = \frac{1}{2}\dot{\mathbf{q}}^T \mathbf{A}\, \dot{\mathbf{q}}.$$

The kinetic energy associated with the mini-manipulator considered alone is

$$T_m = \frac{1}{2}\dot{\mathbf{q}}_m^T \mathbf{A}_m \dot{\mathbf{q}}_m.$$

T_m must be identical to $T(\mathbf{q}, \dot{\mathbf{q}})|_{\dot{\mathbf{q}}_M = 0}$,

$$T(\mathbf{q}, \dot{\mathbf{q}})|_{\dot{\mathbf{q}}_M = 0} = \frac{1}{2}[\, \mathbf{0} \quad \dot{\mathbf{q}}_m^T \,] \begin{bmatrix} \mathbf{A}_{11} & \mathbf{A}_{12} \\ \mathbf{A}_{12}^T & \mathbf{A}_{22} \end{bmatrix} \begin{bmatrix} \mathbf{0} \\ \dot{\mathbf{q}}_m \end{bmatrix} = \frac{1}{2}\dot{\mathbf{q}}_m^T \mathbf{A}_{22} \dot{\mathbf{q}}_m, \tag{40}$$

which implies the identity between $\mathbf{A}_m$ and $\mathbf{A}_{22}$. □

Downloaded from ijr.sagepub.com at Bobst Library, New York University on May 9, 2015

The operational space *pseudo kinetic energy matrix* Λ_0 associated with the linear and angular velocities is defined by $(\mathbf{J}_0\mathbf{A}^{-1}\mathbf{J}_0^T)^{-1}$.

LEMMA 2. The operational space pseudo kinetic energy matrix Λ_0 associated with the macro-/mini-manipulator and the operational space kinetic energy matrix $\Lambda_{m(0)}$ associated with the mini-manipulator are related by

$$\Lambda_0^{-1} = \Lambda_{m(0)}^{-1} + \overline{\Lambda}_C, \tag{41}$$

where

$$\overline{\Lambda}_C = (\mathbf{V}\mathbf{J}_M - \mathbf{J}_m\mathbf{A}_{22}^{-1}\mathbf{A}_{21})\,(\mathbf{A}_{11} - \mathbf{A}_{21}^T\mathbf{A}_{22}^{-1}\mathbf{A}_{21})^{-1} (\mathbf{V}\mathbf{J}_M - \mathbf{J}_m\mathbf{A}_{22}^{-1}\mathbf{A}_{21})^T. \tag{42}$$

Proof. The proof is based on a special matrix decomposition of the kinetic energy matrix **A**. **A** is a symmetric positive definite matrix. The submatrix $\mathbf{A}_{22}$ is nonsingular. Therefore, the matrix **A** can be decomposed (Golub and Van Loan 1983) as

$$\mathbf{A} = \begin{bmatrix} \mathbf{I} & \mathbf{A}_{21}^T\mathbf{A}_{22}^{-1} \\ \mathbf{0} & \mathbf{I} \end{bmatrix} \begin{bmatrix} \overline{\mathbf{A}}_{11}^{-1} & \mathbf{0} \\ \mathbf{0} & \mathbf{A}_{22} \end{bmatrix} \begin{bmatrix} \mathbf{I} & \mathbf{0} \\ \mathbf{A}_{22}^{-1}\mathbf{A}_{21} & \mathbf{I} \end{bmatrix}, \tag{43}$$

where

$$\overline{\mathbf{A}}_{11} = (\mathbf{A}_{11} - \mathbf{A}_{21}^T\mathbf{A}_{22}^{-1}\mathbf{A}_{21})^{-1}. \tag{44}$$

The matrix Λ_0^{-1} is

$$[\mathbf{V}\mathbf{J}_M \quad \mathbf{J}_m] \begin{bmatrix} \mathbf{I} & \mathbf{0} \\ -\mathbf{A}_{22}^{-1}\mathbf{A}_{21} & \mathbf{I} \end{bmatrix} \begin{bmatrix} \overline{\mathbf{A}}_{11} & \mathbf{0} \\ \mathbf{0} & \mathbf{A}_{22}^{-1} \end{bmatrix} \begin{bmatrix} \mathbf{I} & -\mathbf{A}_{21}^T\mathbf{A}_{22}^{-1} \\ \mathbf{0} & \mathbf{I} \end{bmatrix} \begin{bmatrix} \mathbf{J}_M^T\mathbf{V}^T \\ \mathbf{J}_m^T \end{bmatrix}. \tag{45}$$

Substituting $\mathbf{A}_m$ for $\mathbf{A}_{22}$ in the above expression yields equations (41) and (42). □

The inertial properties of the macro-/mini-manipulator are represented by the $m \times m$ matrix, Λ_0. The magnitude of these properties in a direction represented by a unit vector **w** in the m-dimensional space can be described by the scalar

$$\sigma_w(\Lambda_0) = \frac{1}{\mathbf{w}^T\Lambda_0^{-1}\mathbf{w}},$$

which represents the effective inertial properties in the direction **w**.

THEOREM 2. REDUCED INERTIAL PROPERTIES. The operational space pseudo kinetic energy matrices Λ_0 (combined mechanism), and $\Lambda_{m(0)}$ (mini-manipulator) satisfy

$$\sigma_w(\Lambda_0) \leq \sigma_w(\Lambda_{m(0)}), \tag{46}$$

in any direction **w**.

The magnitudes of the inertial properties of the macro-/mini-manipulator system shown in Figure 9, at any configuration and in any direction, are smaller than or equal to the inertial properties associated with the mini-manipulator.

Proof. The proof of this theorem involves the following two steps:

1. *Relationship*. Equation (41) yields,

$$\mathbf{w}^T\Lambda_0^{-1}\mathbf{w} = \mathbf{w}^T\Lambda_{m(0)}^{-1}\mathbf{w} + \mathbf{w}^T\overline{\Lambda}_C\mathbf{w}.$$

This relation can be written as

$$\frac{1}{\sigma_w(\Lambda_0)} = \frac{1}{\sigma_w(\Lambda_{m(0)})} + \alpha,$$

where

$$\alpha = \mathbf{w}^T\overline{\Lambda}_C\mathbf{w}. \tag{47}$$

Completion of the proof requires us to show that $\alpha \geq 0$, that is to show that $\overline{\Lambda}_C$ is a nonnegative definite matrix.

2. *Nonnegative Definition of* $\overline{\Lambda}_C$. Examination of equation (45) shows $\overline{\mathbf{A}}_{11} = (\mathbf{A}_{11} - \mathbf{A}_{21}^T\mathbf{A}_{22}^{-1}\mathbf{A}_{21})^{-1}$ to be the upper diagonal block matrix in the inverse of **A**. $(\mathbf{A}_{11} - \mathbf{A}_{21}^T\mathbf{A}_{22}^{-1}\mathbf{A}_{21})^{-1}$ is thus a positive definite matrix, which can be written as $\mathbf{B}\mathbf{B}^T$. Using this form in the expression of $\overline{\Lambda}_C$ in equation (42) shows that the matrix $\overline{\Lambda}_C$ itself can be written as $\mathbf{C}\mathbf{C}^T$. Substituting this result in equation (47) completes the proof of the theorem. □

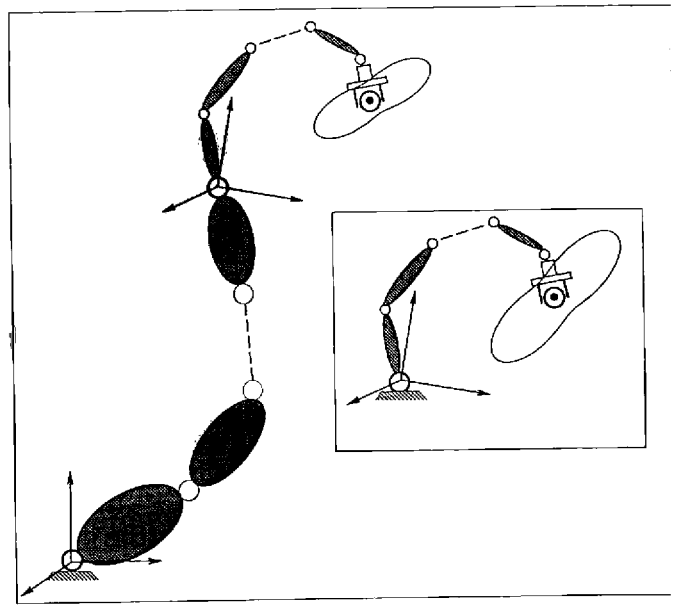

Fig. 9. Inertial properties of a macro-/mini-manipulator.

Downloaded from ijr.sagepub.com at Bobst Library, New York University on May 9, 2015

The reduced effective inertia result obtained for the matrix Λ_0 also applies to the matrices Λ_v and Λ_ω. The matrix Λ_v can be obtained from Λ_0 by replacing the Jacobian $\mathbf{J}_0$ by the matrix

$$\mathbf{J}_v = [\mathbf{I} \quad \mathbf{0}]\mathbf{J}_0. \tag{48}$$

Using equation (48), the decomposition of equation (41) takes the form

$$\Lambda_v^{-1} = \Lambda_{m(v)}^{-1} + \overline{\Lambda}_{C(v)}, \tag{49}$$

where

$$\overline{\Lambda}_{C(v)} = (\mathbf{I} \quad \mathbf{0})\overline{\Lambda}_C \begin{pmatrix} \mathbf{I} \\ \mathbf{0} \end{pmatrix}. \tag{50}$$

This shows that, like $\overline{\Lambda}_C$, the matrix $\overline{\Lambda}_{C(v)}$ is a nonnegative definite matrix. The same procedure can be applied to Λ_ω using

$$\mathbf{J}_\omega = [\mathbf{0} \quad \mathbf{I}]\mathbf{J}_0. \tag{51}$$

COROLLARY 1. REDUCED EFFECTIVE INERTIA. The effective mass (inertia) in (about) any direction $\mathbf{u}$ of a macro-/mini-manipulator system is smaller than or equal to the effective mass (inertia) associated with the mini-manipulator in (about) that direction:

$$m_{\mathbf{u}}(\Lambda_v) \leq m_{\mathbf{u}}(\Lambda_{m(v)}) \quad \text{and} \quad I_{\mathbf{u}}(\Lambda_\omega) \leq I_{\mathbf{u}}(\Lambda_{m(\omega)}), \tag{52}$$

as defined in Section 4.2.

Example. A Three-Degree-of-Freedom Manipulator. Let us consider the three-degree-of-freedom manipulator shown in Figure 10. This manipulator is redundant with respect to the task of positioning the end effector. In this example, the mini-manipulator portion involves two degrees of freedom, $n_m = 2$, and the macro-manipulator portion has only one degree of freedom, $n_M = 1$.

With respect to frame $\mathcal{R}_1$, the Jacobian associated with the end-effector position takes the simple form

$$\mathbf{J}_{0(1)} = \begin{bmatrix} -q_3 & 1 & 0 \\ q_2 & 0 & 1 \end{bmatrix}.$$

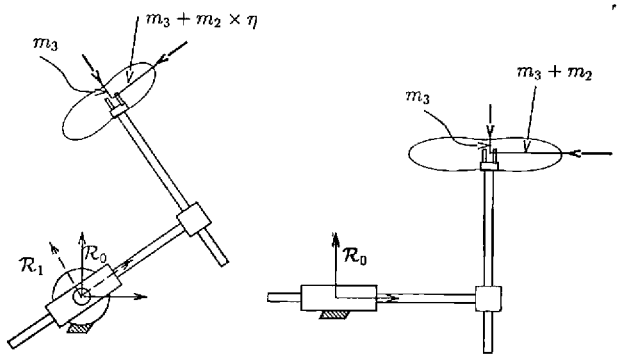

Fig. 10. A 3-DOF manipulator with a 2-DOF mini-manipulator.

The joint-space kinetic energy matrix is

$$\mathbf{A}(\mathbf{q}) = \begin{bmatrix} I_1 + m_2 q_2^2 + m_3(q_2^2 + q_3^2) & -m_3 q_3 & m_3 q_2 \\ -m_3 q_3 & m_2 + m_3 & \mathbf{0} \\ m_3 q_2 & \mathbf{0} & m_3 \end{bmatrix},$$

where I_1 is the inertia of link 1 about joint axis 1 and m_2 and m_3 are the masses of link 2 and link 3. For simplicity we have assumed that the center of mass of link 2 is located at joint axis 3 and the center of mass of link 3 is located at the end effector. The kinetic energy matrix, $\Lambda_{m(0)}$, associated with the two-degree-of-freedom mini-manipulator is

$$\Lambda_{m(0)} = \begin{bmatrix} m_2 + m_3 & 0 \\ 0 & m_3 \end{bmatrix}.$$

In frame $\mathcal{R}_1$, the kinetic energy matrix, $\Lambda_{0(1)}$, associated with the three-degree-of-freedom macro-/mini-manipulator is

$$\Lambda_{0(1)} = \begin{bmatrix} m_2 + m_3 \times \eta & 0 \\ 0 & m_3 \end{bmatrix},$$

where

$$\eta = \frac{I_1 + m_2 q_2^2}{I_1 + m_2(q_2^2 + q_3^2)} \leq 1.$$

The inertial properties of the macro-/mini-manipulator and the mini-manipulator are illustrated in Figure 10. The belted ellipsoids shown in this figure correspond to the eigenvalues and eigenvectors associated with the matrices $\Lambda_{0(1)}$ and $\Lambda_{m(0)}$.

With respect to frame $\mathcal{R}_0$, the kinetic energy matrix, Λ_0 is

$$\Lambda_0 = \Omega \Lambda_{0(1)} \Omega^T;$$

where

$$\Omega = \begin{bmatrix} \cos(q_1) & -\sin(q_1) \\ \sin(q_1) & \cos(q_1) \end{bmatrix}.$$

A more general statement of Theorem 2 is that *the inertial properties of a redundant manipulator are bounded above by the inertial properties of the structure formed by the smallest distal set of degrees of freedom that span the operational space.* The equality of the inertial properties in Theorem 2 is obtained for mechanisms that involve only prismatic joints (Khatib 1990).

5.3. *Dextrous Dynamic Coordination*

The dynamic performance of a macro-/mini-manipulator system can be made comparable to (and, in some cases, better than) that of the lightweight mini-manipulator. The basic idea behind the approach for the coordination of macro and mini structures is to treat them together as a single redundant system. High dynamic performance for

Downloaded from ijr.sagepub.com at Bobst Library, New York University on May 9, 2015

the end-effector task (motion and contact forces) can be achieved with an operational space control system based on equation (23). Minimizing the instantaneous kinetic energy, such a controller will attempt to carry out the entire task using essentially the fast dynamic response of the mini structure. However, given the mechanical limits on the mini structure's joint motions, this would rapidly lead to joint saturation of the mini-manipulator degrees of freedom.

The *dextrous dynamic coordination* we propose is based on combining the operational space control with a minimization of deviation from the midrange joint positions of the mini-manipulator. This minimization must be implemented with joint torque control vectors selected from the dynamically consistent null space of equation (27). This will eliminate any effect of the additional control torques on the end-effector task.

Let $\overline{q}_i$ and $\underline{q}_i$ be the upper and lower bounds on the ith joint position q_i. We construct the potential function

$$V_{\text{Dextrous}}(\mathbf{q}) = k_d \sum_{i=n_M+1}^{n} \left(q_i - \frac{\overline{q}_i + \underline{q}_i}{2} \right)^2, \qquad (53)$$

where k_d is a constant gain. The gradient of this function

$$\boldsymbol{\Gamma}_{\text{Dextrous}} = -\nabla V_{\text{Dextrous}}; \qquad (54)$$

provides the required attraction (Khatib 1986) to the midrange joint positions of the mini-manipulator. The interference of these additional torques with the end-effector dynamics is avoided by projecting them into the null space of $\mathbf{J}^T(\mathbf{q})$. This is

$$\boldsymbol{\Gamma}_{nd} = \left[\mathbf{I}_n - \mathbf{J}^T(\mathbf{q}) \overline{\mathbf{J}}^T(\mathbf{q}) \right] \boldsymbol{\Gamma}_{\text{Dextrous}}. \qquad (55)$$

In addition, joint limit avoidance can be achieved using an "artificial potential field" function (Khatib 1986). It is essential that the range of motion of the joints associated with the mini-manipulator accommodate the relatively slower dynamic response of the arm. A sufficient margin of motion is required to achieve dextrous dynamic coordination.

This approach has been implemented for the coordination and control of a free-flying robotic system (Russakow and Khatib 1992). In the context of this system, several other internal motion behaviors have been proposed for the coordination of the free-flying base, treated as a macro structure, and the manipulator, considered as the relatively lightweight mini structure.

6. Multi-Effector/Object System

We now consider the problem of object manipulation in a parallel system of N manipulators. The effectors are assumed to be rigidly connected to the manipulated object. The number of degrees of freedom of the parallel system will be denoted by n_s.

First, we will consider the case of a system of N nonredundant manipulators that all have the same number of degrees of freedom, n. The end effectors are also assumed to have the same number of degrees of freedom, m ($m = n$). Under these assumptions, the number of degrees of freedom of the parallel system in the planar case ($n = m = 3$) is $n_s = 3$. In the spatial case ($n = m = 6$), this number is $n_s = 6$.

6.1. Augmented Object Model

To analyze the dynamics of this multieffector system, we start by selecting the operational point as a fixed point on the manipulated object. Because of the rigid grasp assumption, this point is also fixed with respect to the end effectors. The number of operational coordinates, m, is equal to the number of degrees of freedom, n_s, of the system. Therefore, these coordinates form a set of generalized coordinates for the system in any domain of the workspace that excludes kinematic singularities. Thus, the kinetic energy of the system is a quadratic form of the generalized operational velocities, $\frac{1}{2}\,\dot{\mathbf{x}}^T \boldsymbol{\Lambda}_{\oplus}(\mathbf{x})\dot{\mathbf{x}}$. The $m \times m$ kinetic energy matrix $\boldsymbol{\Lambda}_{\oplus}(\mathbf{x})$ describes the combined inertial properties of the object and the N manipulators at the operational point. $\boldsymbol{\Lambda}_{\oplus}(\mathbf{x})$ can be viewed as the kinetic energy matrix of an *augmented object* representing the total mass/inertia at the operational point.

Now let $\boldsymbol{\Lambda}_{\mathcal{L}}(\mathbf{x})$ be the kinetic energy matrix associated with the object itself. We will analyze the effect of this load on the inertial properties of a single manipulator and generalize this result to the N-manipulator system to find $\boldsymbol{\Lambda}_{\oplus}(\mathbf{x})$.

6.1.1. Effect of a Load

The kinetic energy matrix $\Lambda(\mathbf{x})$ associated with the operational coordinates $\mathbf{x}$ describes the inertial properties of the manipulator as perceived at the operational point. When the end effector carries a load (see Fig. 11) the system's inertial properties are modified. The addition of a load results in an increase in the total kinetic energy. If we let $m_{\mathcal{L}}$ be the mass of the load and $\mathfrak{I}_{\mathcal{L}(C)}$ be the load inertia matrix evaluated with respect to its center of mass $\mathbf{p}_C$, the additional kinetic energy resulting from the load is

$$T_{\mathcal{L}} = \frac{1}{2} \left(m_{\mathcal{L}} \mathbf{v}_C^T \mathbf{v}_C + \boldsymbol{\omega}^T \mathfrak{I}_{\mathcal{L}(C)} \boldsymbol{\omega} \right), \qquad (56)$$

where $\mathbf{v}_C$ and $\boldsymbol{\omega}_C$ are the linear and angular velocities measured at the center of mass with respect to the fixed reference frame. The kinetic energy matrix associated

Downloaded from ijr.sagepub.com at Bobst Library, New York University on May 9, 2015

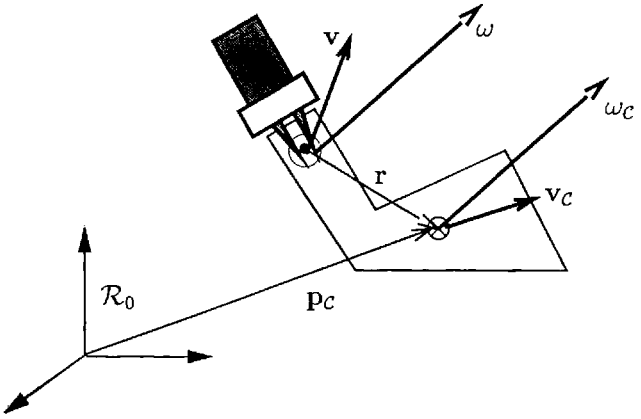

Fig. 11. Center-of-mass/operational-point velocities.

with these velocities is

$$\Lambda_{\mathcal{L}(C)} = \begin{bmatrix} m_{\mathcal{L}}\mathbf{I} & \mathbf{0} \\ \mathbf{0} & \mathfrak{I}_{\mathcal{L}} \end{bmatrix}, \tag{57}$$

where $\mathbf{I}$ and $\mathbf{0}$ are the identity and zero matrices of appropriate dimensions.

To compute the kinetic energy matrix with respect to the operational point, we define $\mathbf{r}$ as the vector connecting the operational point to the object's center of mass $\mathbf{p}_C$. The linear and angular velocities, $\mathbf{v}$ and $\boldsymbol{\omega}$, at the operational point are related to the linear and angular velocities at the center of mass by

$$\begin{bmatrix} \mathbf{v} \\ \boldsymbol{\omega} \end{bmatrix} = \begin{bmatrix} \mathbf{I} & \widehat{\mathbf{r}} \\ \mathbf{0} & \mathbf{I} \end{bmatrix} \begin{bmatrix} \mathbf{v}_C \\ \boldsymbol{\omega}_C \end{bmatrix}, \tag{58}$$

where $\widehat{\mathbf{r}}$ is the cross-product operator associated with vector $\mathbf{r}$. Using the inverse of this relationship, the kinetic energy matrix associated with the load and expressed with respect to the velocities at the operational point can be written as

$$\Lambda_{\mathcal{L}(0)} = \begin{bmatrix} m_{\mathcal{L}}\mathbf{I} & -m_{\mathcal{L}}\widehat{\mathbf{r}} \\ -m_{\mathcal{L}}\widehat{\mathbf{r}}^T & \mathfrak{I}_{\mathcal{L}} + m_{\mathcal{L}}\widehat{\mathbf{r}}^T\widehat{\mathbf{r}} \end{bmatrix}. \tag{59}$$

The generalized operational velocities $\dot{\mathbf{x}}$ are related to the linear and angular velocities by a matrix $\mathbf{E}(\mathbf{x})$. Expressed in terms of operational velocities, the kinetic energy resulting from the load is

$$T_{\mathcal{L}} = \frac{1}{2}\dot{\mathbf{x}}^T\Lambda_{\mathcal{L}}(\mathbf{x})\dot{\mathbf{x}}, \tag{60}$$

where

$$\Lambda_{\mathcal{L}}(\mathbf{x}) = \mathbf{E}^{-T}(\mathbf{x})\Lambda_{\mathcal{L}(0)}\mathbf{E}^{-1}(\mathbf{x}). \tag{61}$$

LEMMA 3. The operational space kinetic energy matrix of the effector and load system is the matrix

$$\Lambda_{\text{effector+load}}(\mathbf{x}) = \Lambda_{\text{effector}}(\mathbf{x}) + \Lambda_{\mathcal{L}}(\mathbf{x}). \tag{62}$$

This is a straightforward implication of evaluation of the total kinetic energy of the system with respect to the operational coordinates.

To extend this result to an N-manipulator system, let $\Lambda_i(\mathbf{x})$ be the kinetic energy matrix associated with the ith unconnected end effector expressed with respect to the operational point.

THEOREM 3. AUGMENTED OBJECT. The kinetic energy matrix of the augmented object is

$$\Lambda_{\oplus}(\mathbf{x}) = \Lambda_{\mathcal{L}}(\mathbf{x}) + \sum_{i=1}^{N}\Lambda_i(\mathbf{x}). \tag{63}$$

This results from the evaluation of the total kinetic energy of the N effectors and object system expressed with respect to the operational velocities,

$$T = \frac{1}{2}\dot{\mathbf{x}}^T\Lambda_{\mathcal{L}}(\mathbf{x})\dot{\mathbf{x}} + \sum_{i=1}^{N}\frac{1}{2}\dot{\mathbf{x}}^T\Lambda_i(\mathbf{x})\dot{\mathbf{x}}$$

The use of the additive property of the augmented object's kinetic energy matrix of Theorem 3 allows us to obtain the system equations of motion from the equations of motion of the individual manipulators. As illustrated in Figure 12, the dynamic behavior of a multieffector/object system is described by the augmented object model

$$\Lambda_{\oplus}(\mathbf{x})\ddot{\mathbf{x}} + \mu_{\oplus}(\mathbf{x},\dot{\mathbf{x}}) + \mathbf{p}_{\oplus}(\mathbf{x}) = \mathbf{F}_{\oplus}. \tag{64}$$

The vector, $\mu_{\oplus}(\mathbf{x},\dot{\mathbf{x}})$, of centrifugal and Coriolis forces also has the additive property

$$\mu_{\oplus}(\mathbf{x},\dot{\mathbf{x}}) = \mu_{\mathcal{L}}(\mathbf{x},\dot{\mathbf{x}}) + \sum_{i=1}^{N}\mu_i(\mathbf{x},\dot{\mathbf{x}}), \tag{65}$$

where $\mu_{\mathcal{L}}(\mathbf{x},\dot{\mathbf{x}})$ and $\mu_i(\mathbf{x},\dot{\mathbf{x}})$ are the vectors of centrifugal and Coriolis forces associated with the object and the ith effector, respectively. Similarly, the gravity vector is

$$\mathbf{p}_{\oplus}(\mathbf{x}) = \mathbf{p}_{\mathcal{L}}(\mathbf{x}) + \sum_{i=1}^{N}\mathbf{p}_i(\mathbf{x}), \tag{66}$$

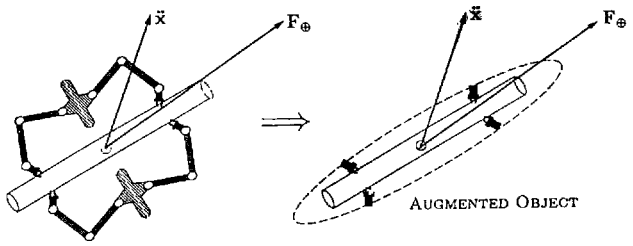

Fig. 12. A multi-arm robot system.

Downloaded from ijr.sagepub.com at Bobst Library, New York University on May 9, 2015

where $\mathbf{p}_{\mathcal{L}}(\mathbf{x})$ and $\mathbf{p}_i(\mathbf{x})$ are the gravity vectors associated with the object and the ith effector. The generalized operational forces $\mathbf{F}_{\oplus}$ are the resultants of the forces produced by each of the N effectors at the operational point.

$$\mathbf{F}_{\oplus} = \sum_{i=1}^{N} \mathbf{F}_i. \tag{67}$$

The effector's operational forces $\mathbf{F}_i$ are generated by the corresponding manipulator actuators. The generalized joint torque vector $\mathbf{\Gamma}_i$ corresponding to $\mathbf{F}_i$ is given by

$$\mathbf{\Gamma}_i = \mathbf{J}_i^T(\mathbf{q}_i)\, \mathbf{F}_i,$$

where $\mathbf{q}_i$ is the vector of joint coordinates associated with the ith manipulator and $\mathbf{J}_i^T(\mathbf{q}_i)$ is the Jacobian matrix of the ith manipulator computed with respect to the operational point. The dynamic decoupling and motion control of the augmented object in operational space is achieved by selecting a control structure similar to that of a single manipulator (Khatib 1987),

$$\mathbf{F}_{\oplus} = \widehat{\mathbf{\Lambda}}_{\oplus}(\mathbf{x})\mathbf{F}^{\star} + \widehat{\boldsymbol{\mu}}_{\oplus}(\mathbf{x}, \dot{\mathbf{x}}) + \widehat{\mathbf{p}}_{\oplus}(\mathbf{x}), \tag{68}$$

where $\widehat{\mathbf{\Lambda}}_{\oplus}(\mathbf{x})$, $\widehat{\boldsymbol{\mu}}_{\oplus}(\mathbf{x}, \dot{\mathbf{x}})$, and $\widehat{\mathbf{p}}_{\oplus}(\mathbf{x})$ represent the estimates of $\mathbf{\Lambda}_{\oplus}(\mathbf{x})$, $\boldsymbol{\mu}_{\oplus}(\mathbf{x}, \dot{\mathbf{x}})$, and $\mathbf{p}_{\oplus}(\mathbf{x})$. With a perfect nonlinear dynamic decoupling, the augmented object (64) under the command (68) becomes equivalent to a *unit mass, unit inertia object*, $\mathbf{I}_m$, moving in the m-dimensional space,

$$\mathbf{I}_m \ddot{\mathbf{x}} = \mathbf{F}^{\star}. \tag{69}$$

Here $\mathbf{F}^{\star}$ is the input to the decoupled system. The control structure for constrained motion and active force control operations is similar to that of a single manipulator.

The control structure (68) provides the net force $\mathbf{F}_{\oplus}$ to be applied to the augmented object at the operational point for a given control input, $\mathbf{F}^{\star}$. Because of the actuator redundancy of multieffector systems, there is an infinity of joint-torque vectors that correspond to this force.

In tasks involving large and heavy objects, a useful criterion for force distribution is minimization of total actuator activities (Khatib 1988). In contrast, dextrous manipulation requires accurate control of internal forces. This problem has received wide attention and algorithms for internal force minimization (Nakamura 1988) and grasp stability (Kumar and Waldron 1988) have been developed. Addressing the problem of internal force in manipulation, we have proposed a physical model, the *virtual linkage* (Williams and Khatib 1993), for the description and control of internal forces and moments in multigrasp tasks. This approach has been used in the manipulation of objects with three PUMA 560 manipulators.

7. Redundancy in Multiarm Systems

When redundant structures are involved in multiarm manipulation, the number of degrees of freedom of the entire system might increase. When this happens, the configuration of the whole system cannot be uniquely described by the set of parameters that specify only the object position and orientation. Therefore, the dynamic behavior of the entire system cannot be described by a dynamic model in operational coordinates. As in the single redundant manipulator case, however, the dynamic behavior of the augmented object itself can still be described, and its equations of motion in operational space can still be established.

The number of *degrees of redundancy* of the multiarm system can be defined by $n_s - m$, where m is the number of degrees of freedom of the augmented object. Obviously, the freedom of the object is restricted by the freedom of the effectors. If m_i is the number of degrees of freedom for the ith effector before connection to the object, the number, m, of degrees of freedom the connected object has will satisfy

$$m \leq \min_i \{m_i\}. \tag{70}$$

The inequality in (70) reflects the fact that additional constraints can be introduced by the connection of effectors.

When the multimanipulator system is redundant (i.e., $n_s > m$), this implies that one or more manipulators must be redundant. In this case, the redundancy of the system can either be localized in one manipulator or distributed between several manipulators. If n_i represents the number of degrees of freedom for the ith manipulator, the number of degrees of redundancy of the ith manipulator is given by $n_i - m$. Only one of the two manipulators in Figure 13*A* is redundant (one degree of redundancy), and both manipulators in Figure 13*B* are redundant (one degree of redundancy each).

7.1. Augmented Object in a Redundant System

To establish the augmented object dynamic model for redundant manipulators, we first determine the number of degrees of freedom of the object, m ($m \leq \min_i\{m_i\}$). The dynamic behavior of the augmented object is then obtained by summing the dynamic properties of the individual manipulators in this m-dimensional operational space. The dynamics of each manipulator will be "projected" into the m-dimensional operational space following the same procedure described for a single redundant manipulator. At this point, the dynamic behavior of each of the effectors will be described by an equation of the form (3). The dynamic behavior of the augmented object system will be given by an equation similar to

Downloaded from ijr.sagepub.com at Bobst Library, New York University on May 9, 2015

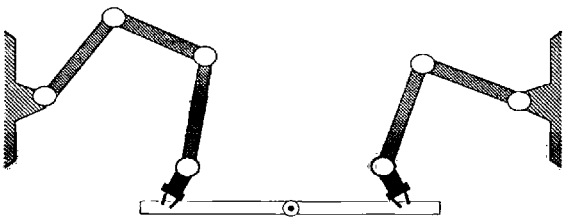

(A) $n_s = 4,\ m = 3$

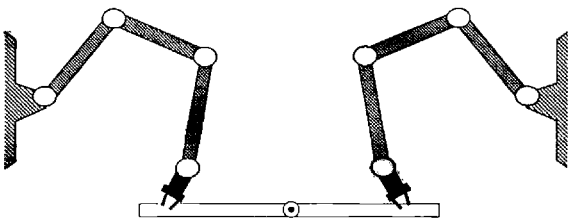

(B) $n_s = 5,\ m = 3$

Fig. 13. Redundancy in multi-arm systems.

equation (64), which was established for the nonredundant multiarm system. In this case, however, the inertial properties of the augmented object are dependent on the full configuration of the system, which is described by

$$\mathbf{q} = (\mathbf{q}_1^T \quad \mathbf{q}_2^T \quad \dots \quad \mathbf{q}_N^T)^T.$$

In this equation, $\mathbf{q}_i$ is the vector of generalized joint coordinates for the ith manipulator. The pseudo kinetic energy matrix of the redundant multiarm system is

$$\mathbf{\Lambda}_{\oplus}(\mathbf{q}) = \mathbf{\Lambda}_{\mathcal{L}}(\mathbf{x}) + \sum_{i=1}^{N} \mathbf{\Lambda}_i(\mathbf{q}_i). \tag{71}$$

Dynamic decoupling and control of the multieffector/object system can be achieved by selecting the same control structure (68) used in the nonredundant case. However, as in the case of a single redundant manipulator, dynamics in the null spaces associated with the redundant manipulators must be calculated and controlled. This requires the identification of dynamically consistent relationships between joint torque vectors and end-effector operational forces.

7.2. *Dynamic Consistency in Multiarm Systems*

In the case of a single redundant manipulator, we have seen that the general relationship between joint torques and end-effector forces is based on the use of a dynamically consistent generalized inverse of the Jacobian transpose. For a single manipulator, this inverse is given (see equation (22)) by

$$\bar{\mathbf{J}}(\mathbf{q}) = \mathbf{A}^{-1}(\mathbf{q})\mathbf{J}^T(\mathbf{q})\mathbf{\Lambda}(\mathbf{q}).$$

The extension of this relationship to redundant multiarm systems is complicated by the fact that the dynamically consistent generalized inverse is dependent on the joint-space kinetic energy matrix $\mathbf{A}(\mathbf{q})$. The joint-space kinetic energy matrix of a redundant manipulator in a multiarm system is not simply the matrix associated with the unconnected manipulator considered alone. Connection of the manipulator to an object results in increased loading on the effector of this manipulator. This load, which is due to the object and all the other manipulators connected to it, affects the kinetic energy matrix of this manipulator.

To analyze this, we will first examine how the joint-space kinetic energy matrix in the case of a single manipulator is affected by the addition of a simple load.

7.2.1. *Effect of a Load on a Single Manipulator*

The addition of a load to the effector of a single manipulator will result in an increase in the kinetic energy of the system. Let $\mathbf{\Lambda}_{\text{load}}(\mathbf{x})$ be the kinetic energy matrix associated with the load and expressed with respect to the operational point.

LEMMA 4. The joint-space kinetic energy matrix of a manipulator with load is the matrix

$$\mathbf{A}_{\text{arm+load}}(\mathbf{q}) = \mathbf{A}_{\text{arm}}(\mathbf{q}) + \left[\mathbf{J}^T(\mathbf{q})\mathbf{\Lambda}_{\text{load}}(\mathbf{x})\mathbf{J}(\mathbf{q})\right]. \tag{72}$$

This result is derived by expressing the total kinetic energy of the combined arm-load system in joint space:

$$\begin{aligned} T &= \frac{1}{2}\left[\dot{\mathbf{q}}^T\mathbf{A}(\mathbf{q})\dot{\mathbf{q}} + \dot{\mathbf{x}}^T\mathbf{\Lambda}_{\text{load}}(\mathbf{x})\dot{\mathbf{x}}\right] \\ &= \frac{1}{2}\dot{\mathbf{q}}^T\left[\mathbf{A}(\mathbf{q}) + \mathbf{J}^T(\mathbf{q})\mathbf{\Lambda}_{\text{load}}(\mathbf{x})\mathbf{J}(\mathbf{q})\right]\dot{\mathbf{q}}. \end{aligned} \tag{73}$$

7.2.2. *Reflected Load*

The pseudo kinetic energy matrix $\mathbf{\Lambda}_{\oplus}(\mathbf{q})$ describes the inertial characteristics of the N-effector/object system as reflected at the operational point. Viewed from a given manipulator, the object and the other effectors can be seen as a load attached to its effector. The additional load perceived by the ith manipulator is $\mathbf{\Lambda}_{\oplus}(\mathbf{q}) - \mathbf{\Lambda}_i(\mathbf{q}_i)$, as illustrated in Figure 14. Following Lemma 4, the kinetic energy matrix of the manipulator resulting from this additional load is

$$\mathbf{A}_{+_i}(\mathbf{q}) = \mathbf{A}_i(\mathbf{q}_i) + \mathbf{J}_i^T(\mathbf{q}_i)\left[\mathbf{\Lambda}_{\oplus}(\mathbf{q}) - \mathbf{\Lambda}_i(\mathbf{q}_i)\right]\mathbf{J}_i(\mathbf{q}_i). \tag{74}$$

THEOREM 4. DYNAMIC CONSISTENCY IN A MULTIARM SYSTEM. The generalized inverse associated with the ith

Downloaded from ijr.sagepub.com at Bobst Library, New York University on May 9, 2015

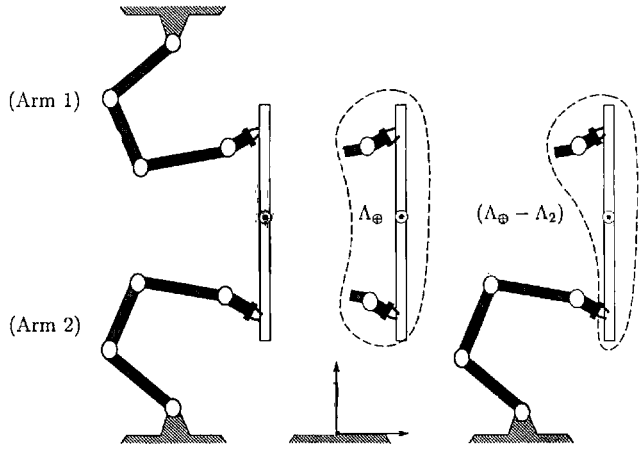

Fig. 14. Reflected load.

manipulator and consistent with the dynamic behavior of the multieffector/object system is

$$\bar{\mathbf{J}}_i(\mathbf{q}) = \mathbf{A}_+^{-1}(\mathbf{q})\mathbf{J}_i^T(\mathbf{q}_i)\left[\mathbf{J}_i(\mathbf{q}_i)\mathbf{A}_+^{-1}(\mathbf{q})\mathbf{J}_i^T(\mathbf{q}_i)\right]^{-1}. \quad (75)$$

Finally, the joint torque end-effector force relationship for the ith manipulator is

$$\mathbf{\Gamma}_i = \mathbf{J}_i^T(\mathbf{q}_i)\mathbf{F}_i + \left[\mathbf{I}_n - \mathbf{J}_i^T(\mathbf{q}_i)\bar{\mathbf{J}}_i^T(\mathbf{q})\right]\mathbf{\Gamma}_{i_0}, \quad (76)$$

where $\mathbf{\Gamma}_{i_0}$ is an arbitrary joint-torque vector. Asymptotic stabilization (Khatib 1987), dextrous dynamic coordination, link collision avoidance (Khatib 1986), and control of manipulator postures can all be integrated in the vector $\mathbf{\Gamma}_{i_0}$, which causes no acceleration at the operational point.

8. Summary and Discussion

This article has presented a study of dynamics and control for robotic systems involving redundant series and parallel kinematic structures. A distinctive characteristic of this study is its focus on mathematical models and control strategies that relate to the behavior of the object being manipulated.

The analysis of inertial properties perceived at the manipulated object has resulted in two models: an effective mass that describes the dynamic response to a contact force or for a translational motion, and an effective inertia that describes the response to a moment or for a rotational motion. To visualize the effective mass and inertia, we have proposed a new geometric representation, the belted ellipsoid, that provides a display of the actual magnitudes of these properties.

Macro-/mini-manipulators are redundant series structures. The description of the dynamic behavior of the manipulated object in a redundant structure has been obtained by a projection of the system's dynamics into the operational space. Control of the remainder of the dynamics, which affects joint motions in the null space, is achieved by formulating a dynamically consistent relationship between joint torques and end-effector forces. With this relationship, joint torques are decomposed into two dynamically decoupled control vectors: joint torques corresponding to forces acting at the end effector and joint torques that only affect internal motions. Using this decomposition, the end effector can be independently controlled by operational forces, whereas internal motions can be controlled by joint torques that are guaranteed not to alter the end effector's dynamic behavior. In addition to their impact on the control of redundant manipulators, these models have been the basis for the development of an effective strategy for dealing with kinematic singularities. With this strategy, a manipulator at a singular configuration is treated as a redundant system in the subspace orthogonal to the singular direction. This strategy has been implemented for a PUMA 560 manipulator in operations involving multiple singularities.

Our analysis of inertial properties for macro-/mini-manipulator systems has shown that for all directions and configurations, the effective mass/inertia of a macro-/mini-manipulator is smaller than or equal to the inertia associated with the mini-manipulator structure, considered alone. To allow the mini-structure's high bandwidth to be fully utilized in wide range operations, we have proposed a dextrous dynamic coordination strategy that uses the system's internal motions to minimize deviation from the midrange joint positions of the mini-manipulator. Effective implementation of this strategy relies on preventing any effects of the internal motion from influencing the primary end-effector task. This is achieved by using the dynamically consistent relationship between joint torques and end-effector forces.

The dextrous dynamic coordination can be quite simply extended to the coordination of holonomic mobile manipulator platforms. A mobile manipulator system can be viewed as the mechanism resulting from the serial combination of two subsystems: a macro structure with coarse, slow, dynamic responses (the mobile base), and a relatively fast and accurate mini device (the manipulator). The results obtained for fixed-base redundant manipulation systems directly extend to holonomic mobile manipulator systems. This approach has been implemented for the coordination and control of a free-flying robotic system (Russakow and Khatib 1992).

Analyzing the inertial properties of multiarm robot systems, we have presented an important additive property of parallel structures. It has been shown that the inertial properties perceived at the manipulated object are given by the sum of the inertial properties associated with each individual manipulator and the inertial properties of the unconstrained object, all expressed with respect to the

Downloaded from ijr.sagepub.com at Bobst Library, New York University on May 9, 2015

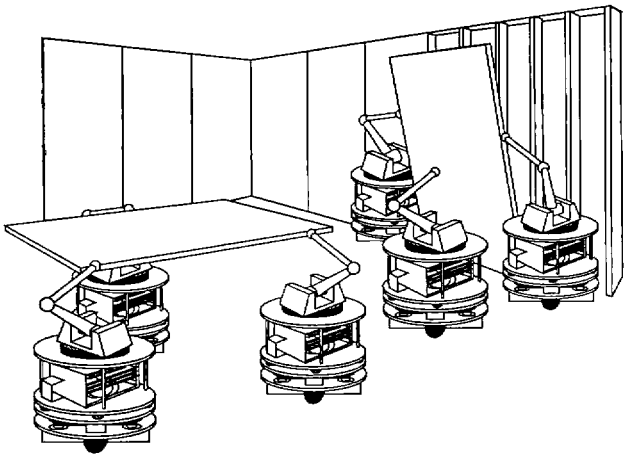

Fig. 15. Robotics in construction: Drywall.

same operational point. Centrifugal, Coriolis, and gravity forces have also been shown to possess this additive property. Combining the dynamics of the individual manipulators and object, we have proposed the *augmented object* as a model of the dynamics at the operational point for the multi-arm robot system. This approach has been implemented for object manipulation involving two and three PUMA 560 manipulators (Williams and Khatib 1993). In these implementations, the description and control of internal forces and moments have been based on the virtual linkage model.

The augmented object model and the dynamically consistent force/torque relationship have been extended for multiarm systems involving redundancy. We are currently using these models in conjunction with the dextrous dynamic coordination strategy for cooperative operations between multiple vehicle/arm systems in construction tasks, as illustrated in Figure 15.

By providing object-level models of robot dynamics, the operational space framework overcomes many of the deficiencies associated with joint-space formulations. It is important to emphasize the fact that the performance of operational space implementations relies on the robot's ability to achieve effective control of joint torques. This capability is, in fact, a key requirement for any dynamic control implementation—including joint-space implementations.

Acknowledgments

The financial support of Boeing, General Motors, Hitachi Construction Machinery, and Toyota Motors is gratefully acknowledged. Many thanks to Harlyn Baker, Alan Bowling, Roy Featherstone, Leo Guibas, Robert Holmberg, Sean Quinlan, and David Williams for their comments and help during the preparation of the manuscript.

References

Alford, C. O., and Belyeu, S. M. 1984. Coordinated control of two robot arms. *Proc. IEEE Int. Conference on Robotics and Automation,* Atlanta, GA, pp. 468–473.

Asada, H., 1983. A geometrical representation of manipulator dynamics and its application to arm design. *Trans. ASME J. Dynamic Sys. Measurement Control* 105(3):131–135.

Cai, C.-H., and Roth, B. 1987. Impact sensitivity to mass distribution of a planar manipulator. *Proc. ICAR: 3rd Int. Conf. Advanced Robotics*, Versailles, France, pp. 115–124.

Golub, G. H., and Van Loan, C. F. 1983. *Matrix Computations*. Baltimore, MD: The Johns Hopkins University Press.

Hammer, R., Hollis, L., An, C. H., and Hendricks, F. 1992. Design and control of an air-bearing supported three-degree-of-freedom fine positioner. *Proc. IEEE Int. Conference on Robotics and Automation,* Nice, France, pp. 677–684.

Hayati, S. 1986. Hybrid position/force control of multi-arm cooperating robots. *Proc. IEEE Int. Conference on Robotics and Automation,* San Francisco, CA, pp. 1375–1380.

Hogan, N. 1984. Impedance control of industrial robots. *Robotics Computer-Integrated Manufacturing* 1(1):97–113.

Hollis, R. 1985. A planar XY robotics fine positioning device. *Proc. IEEE Int. Conference on Robotics and Automation,* St. Louis, MO, pp. 329–337.

Karidis, J. P., McVicker, G., Pawletko, J. P., and Zai, L. C. 1992. The hummingbird minipositioner—providing three axis motion at 50 G's with low reactions. *Proc. IEEE Int. Conference on Robotics and Automation,* Nice, France, pp. 685–692.

Khatib, O. 1980. *Commande Dynamique dans l'Espace Opérationnel des Robots Manipulateurs en Présence d'Obstacles*. Thése de Docteur-Ingénieur. École Nationale Supérieure de l'Aéronautique et de l'Espace, Toulouse, France.

Khatib, O. 1986. Real-time obstacle avoidance for manipulators and mobile robots. *Int. J. Robot. Res.* 5(1): 90–98.

Khatib, O. 1987. A unified approach to motion and force control of robot manipulators: The operational space formulation. *IEEE J. Robot. Automation* 3(1):43–53.

Khatib, O. 1988. Object manipulation in a multi-effector robot system. In Bolles, R., and Roth, B. (eds.): *Robotics Research 4*. Cambridge, MA: MIT Press, pp. 137–144.

Khatib, O. 1990. Reduced effective inertia in macro/mini-manipulator systems. In Miura, H., and Arimoto, S. (eds.): *Robotics Research 5*. Cambridge, MA: MIT Press, pp. 279–284.

Downloaded from ijr.sagepub.com at Bobst Library, New York University on May 9, 2015

Khatib, O., and Agrawal, S. 1989. Isotropic and uniform inertial and acceleration characteristics: Issues in the design of manipulators. In Schweitzer, G., and Mansour, M. (eds.): *Dynamics of Controlled Mechanical Systems*. New York: Springer-Verlag, pp. 259–270.

Khatib, O., and Burdick, J. 1985. Dynamic optimization in manipulator design: The operational space formulation. In Donath, M., and Leu, M. (eds.): *Robotics and Manufacturing Automation*. Proc. ASME Winter Annual Meeting, Miami, Vol. 15, pp. 169–174.

Kumar, V., and Waldron, K. J. 1988. Force distribution in closed kinematic chains. *Proc. IEEE Int. Conference on Robotics and Automation,* Philadelphia, PA, pp. 114–119.

Kumar, V., Yun, X., Paljug, E., and Sarkar, N. 1991. Control of contact conditions for manipulation with multiple robotic systems. *Proc. IEEE Int. Conference on Robotics and Automation,* Sacramento, CA, pp. 170–175.

Luh, J. Y. S., Walker, M. W., and Paul, P. 1980. Resolved acceleration control of mechanical manipulators. *IEEE Trans. Auto. Control* 25(3):468–474.

Merlet, J. P. 1988. Force-feedback control of parallel manipulators. *Proc. IEEE Int. Conference on Robotics and Automation,* Philadelphia, PA, pp. 1484–1489.

Nakamura, Y. 1988. Minimizing object strain energy for coordination of multiple robotic mechanisms. *Proc. American Control Conference,* pp. 499–504.

Reboulet, C., and Robert, A. 1986. Hybrid control of a manipulator equipped with an active compliant wrist. In Faugeras, O., and Giralt, G. (eds.): *Robotics Research: 3rd International Symposium*. Cambridge, MA: MIT Press, pp. 237–241.

Russakow, J., and Khatib, O. 1992. A new control structure for free-flying space robots. *International Symposium on Artificial Intelligence, Robotics and Automation in Space,* Toulouse, France, pp. 395–403.

Sharon, A., Hogan, N., and Hardt, D. 1988. High bandwidth force regulation and inertia reduction using a macro-/micro manipulator system. *Proc. IEEE Int. Conference on Robotics and Automation,* Philadelphia, PA, pp. 126–132.

Takase, K. 1977. Task-oriented variable control of manipulator and its software servoing system. *Proc. IFAC Int. Symp.,* pp. 139–145.

Tarn, T. J., Bejczy, A. K., and Yun, X. 1987. Design of dynamic control of two cooperating robot arms: Closed chain formulation. *Proc. IEEE Int. Conference on Robotics and Automation,* Raleigh, NC, pp. 7–13.

Tilley, S. W., Cannon, R. H., and Kraft, R. 1986. End-point force control of a very flexible manipulator with a fast end-effector. *Proc. ASME Winter Annual Meeting,* Anaheim, CA, Vol. 3, pp. 1–9.

Uchiyama, M., and Dauchez, P. 1988. A symmetric hybrid position/force control scheme for the coordination of two robots. *Proc. IEEE Int. Conference on Robotics and Automation,* Philadelphia, PA, pp. 350–356.

Williams, D., and Khatib, O. 1993. The virtual linkage: A model for internal forces in multi-grasp manipulation. *Proc. IEEE Int. Conference on Robotics and Automation,* Atlanta, GA, pp. 1025–1030.

Williams, D., and Khatib, O. 1993. Experiments in multi-arm manipulation. *Preprints of the Third International Symposium on Experimental Robotics (ISER 3),* Kyoto, Japan, pp. 321–330.

Zheng, Y. F., and Luh, J. Y. S. 1986. Joint torques for control of two coordinated moving robots. *Proc. IEEE Int. Conference on Robotics and Automation,* San Francisco, CA, pp. 1375–1380.

Downloaded from ijr.sagepub.com at Bobst Library, New York University on May 9, 2015